

Growth-related Mutational Effects and Phenotypic Evolution in

*Escherichia coli*

by

Jadon Gonzales

A Thesis Presented in Partial Fulfillment  
of the Requirements for the Degree  
Master of Science

Approved April 2023 by the  
Graduate Supervisory Committee:

Michael Lynch, Chair  
Kerry Geiler-Samerotte  
Wei-Chin Ho

ARIZONA STATE UNIVERSITY

May 2023

## ABSTRACT

Phenotypic evolution is of great significance within biology, as it is the culmination of the influence of key evolutionary factors on the expression of genotypes. Deeper studies of the fundamental components, such as fitness effects of mutations and genetic variance within a population, allow one to predict the evolutionary trajectory of phenotypic evolution. In this regard, how much the change in mutational variance and the ongoing natural selection influence the rate of phenotypic evolution has yet to be fully understood. Therefore, this study measured mutational variances and the increasing rate of genetic variance during the experimental evolution of *Escherichia coli* populations, focusing on two growth-related traits, the populational maximum growth rate and carrying capacity. Mutational variances were measured by mutation-accumulation experiments, which allowed for the analysis of the effects of spontaneous mutations on growth-related traits in the absence of selection. This analysis revealed that some evolved populations developed a higher mutational variance for growth-related traits. Further investigation showed that most evolved populations have also developed a greater mutational effect, which could explain the increase in mutational variance. Finally, the genetic variances for most evolved populations are lower than expected in the absence of selection, and the involvement of either stabilizing or directional selection is evident. Future experiments with a larger sample size of experimentally evolved populations, as well as more intermediate timepoints during experimental evolution, may provide further insight regarding the complexities of the evolutionary outcomes of these traits.

## TABLE OF CONTENTS

	Page
LIST OF FIGURES.....	iv
INTRODUCTION.....	1
RESULTS.....	6
Evolution of Mutational Variance During Experimental Evolution.....	6
Evolution of Mutational Variance During Experimental Evolution.....	6
Expectation of Mutational Effects.....	14
Expectation of Square Mutational Effects.....	20
Response of Genetic Variance to Experimental Evolution.....	26
DISCUSSION.....	33
Evolution of Mutational Variance During Experimental Evolution.....	33
Expectation of Mutational Effects.....	33
Expectation of Square Mutational Effects.....	34
Response of Genetic Variance to Experimental Evolution.....	35
Limitations.....	36
Future Studies.....	38
METHODS.....	39
Populations.....	39
Growth Curves.....	40
Statistical Analysis.....	41
REFERENCES.....	43

APPENDIX

Page

A SUPPLEMENTARY TABLES.....45

## LIST OF FIGURES

Figure	Page
1. Comparison of Mutational Variance of $\mu_{\max}$ Between WT Ancestor-derived MA Experiments and WT Evolved Population-derived MA Experiments.....	10
2. Comparison of Mutational Variance of $\mu_{\max}$ Between MMR- Ancestor-derived MA Experiments and MMR- Evolved Population-derived MA Experiments.....	11
3. Comparison of Mutational Variance of $K_c$ Between WT Ancestor-derived MA Experiments and WT Evolved Population-derived MA Experiments.....	12
4. Comparison of Mutational Variance of $K_c$ Between MMR- Ancestor-derived MA Experiments and MMR- Evolved Population-derived MA Experiments.....	13
5. Expectation of Mutational Effects on $\mu_{\max}$ Within the WT Ancestor and WT Evolved Populations.....	16
6. Expectation of Mutational Effects on $\mu_{\max}$ Within the MMR- Ancestor and MMR- Evolved Populations.....	17
7. Expectation of Mutational Effects on $K_c$ Within the WT Ancestor and WT Evolved Populations.....	18
8. Expectation of Mutational Effects on $K_c$ Within the MMR- Ancestor and MMR- Evolved Populations.....	19
9. Expectation of Square Mutational Effects on $\mu_{\max}$ Within the WT Ancestor and WT Evolved Populations.....	22
10. Expectation of Square Mutational Effects on $\mu_{\max}$ Within the MMR- Ancestor and MMR- Evolved Populations.....	23

Figure	Page
11. Expectation of Square Mutational Effects on $K_c$ Within the WT Ancestor and WT Evolved Populations.....	24
12. Expectation of Square Mutational Effects on $K_c$ Within the MMR- Ancestor and MMR- Evolved Populations.....	25
13. Accumulation Rate of Genetic Variance of $\mu_{\max}$ Among WT Evolved Populations....	29
14. Accumulation Rate of Genetic Variance of $\mu_{\max}$ Among MMR- Evolved Populations. .....	30
15. Accumulation Rate of Genetic Variance of $K_c$ Among WT Evolved Populations.....	31
16. Accumulation Rate of Genetic Variance of $K_c$ Among MMR- Evolved Populations..	32

## **Introduction**

The study of phenotypic evolution is an important component of evolutionary biology as it allows one to observe the expression of a given trait and how it changes over time in response to various evolutionary mechanisms such as mutation and selection (Stern and Orgogozo 2008; Stern and Orgogozo 2009; Orr 1998). The factors changing a phenotype comprise a genetic and environmental component, and often involve interactions between the two (West-Eberhard 1989; Scheiner 1993; Pigliucci 2001; Pigliucci 2005; Aubin-Horth and Renn 2009). Because the genetic basis of phenotypic changes is one of the foundations allowing natural selection to work in populations, it is of great interest in the field of evolutionary biology (Stern and Orgogozo 2008; Stern and Orgogozo 2009; McGuigan 2006; Wray 2013). When the influence of the environmental component is minimized, any significant changes in phenotype can typically be attributed to a change in the genetic component.

The underlying structure of the genetic source in the phenotypic outcome differs between traits, with quantitative traits demonstrating a high degree of complexity (Mackay 2001; Neher and Boris 2011; Lynch and Walsh 1998). The non-discrete nature of quantitative traits allows for a variety of potential phenotypic values. As such, the individuals within a given population can display a range of phenotypic values. The variation among the individuals of a population typically results in a normal distribution of phenotypes (Fisher 1918; Barton, Etheridge, and Véber 2017). Evolutionary forces can influence these phenotypic distributions, causing them to shift over time. Of particular interest is the form of distribution shift, as it may indicate what primary evolutionary mechanisms are influencing these phenotypic changes. Identifying the form of

phenotypic distribution shift in a population with known environmental and demographic factors can enhance one's knowledge on how those underlying factors shape the evolutionary trajectory of phenotypes in the population.

One aspect one can track in the evolutionary trajectory of a population is the genetic variance, which is subject to change by selection. For example, stabilizing selection describes a scenario in which intermediate trait values display greater fitness compared to extreme trait values. Under this mode of selection, the distribution of phenotypic trait values within a given population shifts in response to selection, resulting in a deficit of genetic variance. Directional selection is another mode of selection that depicts a scenario in which one extreme of the potential phenotypic trait values is most favorable, in terms of fitness. Directional selection is associated with a phenotypic distribution shift that often results in a slight deficit of genetic variance. The third mode of selection, disruptive selection, portrays a scenario in which both extremes display greater fitness compared to the intermediate trait values. The phenotypic distribution shift caused by disruptive selection results in an excess of genetic variance. Successfully identifying the mode of selection influencing a phenotype within a population can be useful when making predictions regarding the fate of that phenotype in the future.

Phenotypic traits are expected to evolve over time due to the accumulation of mutations across generations, even in the relative absence of selection (Lande 1976; Lynch and Hill 1986; Zhang 2018). Mutations can have a wide range of potential fitness effects, ranging from deleterious to beneficial, by varying fitness-related phenotypes (Eyre-Walker and Keightley 2007; Loewe and Hill 2010; Bataillon and Bailey 2014). Under selection, strongly deleterious mutations typically see a rapid decrease in

frequency over time, eventually leading to the extinction of that allele, while beneficial, neutral, and even slightly deleterious mutations typically persist for a longer duration, and may eventually become fixed within the population. This can result in phenotypic distribution shifts resembling the modes of selection previously mentioned. However, when the influence of competing evolutionary forces such as genetic drift minimize the effective strength of selection, a wider range of mutations are able to persist within a population (Kimura 1979; Kimura 1991; Ohta 1992). In this scenario, the fates of these mutations are less deterministic, but can result in significant phenotypic distribution shifts. This highlights the importance of determining whether a shift in the phenotypic distribution is caused primarily by selection acting upon that particular phenotype or if it can be adequately explained by the evolution of mutational effects. In order to make this distinction, it would be necessary to analyze the distribution of fitness effects of spontaneous mutations in addition to the phenotypic distribution, as a significant difference between the two distributions may indicate that the phenotype is under selection.

The goal of this study was to utilize the information provided by the phenotypic distribution and the distribution of mutational effects to make inferences regarding the evolution of growth-related traits in *E. coli* populations. Furthermore, this study sought to investigate whether the evolutionary mode in growth-related traits is affected by the genetic background and effective population size ( $N_e$ ). To accomplish this, this study utilized seven experimentally evolved populations of *E. coli* (Ho, et al. 2021; Wei, et al. 2022), differentiated based on their genetic background and  $N_e$ . The genetic background of each population was classified according to the ancestor from which the population

was derived. Three of the evolved populations were derived from the wildtype (WT) ancestor, which is associated with a relatively low mutation rate. The other four evolved populations were derived from the mismatch repair knockout (MMR-) ancestor, which is associated with a relatively high mutation rate due to the knockout of the mismatch repair gene. The  $N_e$  of each population was classified according to the daily transfer size that the population was subjected to during experimental evolution, with a large transfer size resulting in a relatively large  $N_e$ , and a small transfer size resulting in a relatively small  $N_e$ . This study focused on two growth-related traits, maximum growth rate and carrying capacity, as the primary phenotypes to be investigated.

The first step in investigating the evolution of growth-related traits in the populations was to study the evolution of mutational effects within each population. This was accomplished by utilizing mutation-accumulation data to calculate the mutational variance, a key parameter for predicting phenotypic outcomes, particularly the accumulation rate of genetic variance, in the absence of selection. The mutational variance was calculated for each population before and after experimental evolution to reveal how it has changed between the two timepoints.

After analyzing the changes in mutational variance during experimental evolution, the next step was to verify whether these changes in mutational variance could be adequately explained by changes in mean mutational effect size during experimental evolution, or if there was an alternate explanation worth investigating. This was done by calculating the mean fitness effect size of spontaneous mutations within each population using mutation-accumulation data. The change in mean effect size was observed by comparing the results for the timepoints before and after experimental evolution. The

results of this analysis were then compared to the mutational variance results to identify common trends.

In addition to the mean mutational effect size, this study sought to investigate the evolution of mutational effects on genetic variance, and whether this contributed to the changes in mutational variance during experimental evolution. This was done by utilizing the previous mutational variance results, and the mutational data for each population to calculate the genetic variance per spontaneous mutation before and after experimental evolution. The results of this analysis were also compared to the mutational variance results to identify commonalities.

The final step was to calculate the accumulation rate of genetic variance for each evolved population and compare the results to the mutational variance results that were calculated previously. Because mutational variance allows one to predict the expected accumulation rate of genetic variance in the absence of selection, any significant deviation from this expectation could be considered evidence for the involvement of selection in the evolution of these growth-related traits. Thus, this comparison revealed which populations' growth-related traits showed evidence of selection, what mode of selection the changes in variance resemble, and whether there are observable trends based on the genetic background and  $N_e$ .

## Results

### Experimentally Evolved Populations

This study utilized seven experimentally evolved *E. coli* populations that have experienced different transfer schemes and originated from different ancestors. These populations are labeled as “x1-y”. The *x* label corresponds to the population’s daily transfer scheme, with “L” indicating a large transfer scheme (1/10 volume transferred), and “S” indicating a small transfer scheme (1/10<sup>7</sup> volume transferred). The *y* label corresponds to the population’s experimental evolution ancestor, with “A” and “B” indicating two independent populations evolved from the MMR- ancestor, and “C” and “D” indicating two independent populations evolved from the WT ancestor. MMR- ancestors show approximately 100-fold higher mutation rates compared to WT ancestors. Categorizing the evolved populations based on their ancestor and transfer scheme allows for an analysis of the influence of genetic background and  $N_e$  on growth-related mutational and phenotypic outcomes, which is the goal of this study.

### Evolution of Mutational Variance During Experimental Evolution

Mutation is a critical component of phenotypic evolution. In order to fully analyze how growth-related traits have evolved in the *E. coli* populations during experimental evolution, it was first necessary to investigate the evolution of mutational effects within these populations. One key component associated with the evolution of mutational effects is the mutational variance ( $V_m$ ), or the change of variance due to spontaneous mutations (i.e., no selection) per generation. In theory,  $V_m$  serves as a critical parameter for predicting the expected genetic variance of a trait given that no selection is involved in

the evolution of that trait.  $V_m$  can thus be utilized as the null expectation when investigating the influence selection on a particular trait, which is a goal of this study.

Because  $V_m$  is defined as the change in variance due to spontaneous mutations, selection must be accounted for when measuring  $V_m$  within a population. The influence of selection creates a bias regarding which mutations are able to persist in a population, which interferes with the ability to accurately measure the effects of spontaneous mutations, especially after a long period of time. Therefore, the influence of selection must be minimized in order to measure  $V_m$ .

Specifically, this study utilized mutation-accumulation (MA) experiments derived from the target populations. These MA experiments typically involve 60 days of daily transfers of a single random colony. Because the MA process involves the transfer of only a single colony, chosen at random, the influence of selection on these MA experiments is minimized, allowing for the calculation of  $V_m$ .

This study first utilized MA experiments derived from the day-0 WT and MMR-ancestors to calculate  $V_m$ . Growth curves were collected for up to 42 replicate MA lines derived from the same progenitor, with up to 16 replicates for each MA line. The phenotypic values of the maximum growth rate ( $\mu_{max}$ ) and carrying capacity ( $K_c$ ) traits were determined in each growth curve. After collecting all of the phenotypic data, an analysis of variance (ANOVA) was used to partition the different portions of variances of the  $\mu_{max}$  and  $K_c$  traits, including the among-line component ( $V_L$ ) and the residual environmental component ( $V_E$ ) for each MA experiment. Using  $V_L$  and the total generation number in the MA process ( $g$ ),  $V_m$  was estimated by  $2V_L/g$  (Lynch and Walsh 1998) for each MA experiment.

In addition to using day-0 WT and MMR- ancestors as the progenitors for the MA experiments, the isolates from experimentally evolved populations were also used as progenitors of MA experiments, as comparing the two sets of MA experiments would reveal whether there was evolution of mutational features during experimental evolution. In particular, the  $V_m$  of the evolved population-derived MA experiments were then compared to the  $V_m$  of the corresponding ancestor-derived MA experiment.

In the analysis with  $\mu_{max}$ , of the five WT evolved population-derived MA experiments, three display a significant increase in  $V_m$  compared to the WT ancestor-derived MA experiment: MA experiments L1-D1, L1-D2, and S1-C2 (**Figure 1**). For the MMR- MA experiments, only one of the four evolved population-derived MA experiments, L1-A1, displays a significant increase in  $V_m$  compared to the MMR- ancestor-derived MA experiment (**Figure 2**).

For the analysis with the  $K_c$  trait, two of the five WT evolved population-derived experiments, L1-D1 and S1-C2, demonstrate a significant increase in  $V_m$  compared to the WT ancestor-derived MA experiment (**Figure 3**). For the MMR- MA experiments, two of the four evolved population-derived MA experiments, L1-A1 and S1-B1, show a significant increase in  $V_m$  compared to the MMR- ancestor-derived MA experiment (**Figure 4**).

These results show that several of the populations – L1-D, S1-C, L1-A, and S1-B – display an increase in  $V_m$  after 1000 days of experimental evolution compared to the day-0 ancestral state. This suggests that the mutational effects on  $\mu_{max}$  and  $K_c$  have evolved during experimental evolution. However, the results show minimal distinction based on genetic background and  $N_e$ , as populations of both the WT and MMR-

backgrounds, as well as the Large and Small transfer sizes, display this increase in  $V_m$ . Thus, there is not enough evidence to conclude that genetic background and  $N_e$  significantly influence the evolution of  $V_m$  of  $\mu_{\max}$  and  $K_c$ .

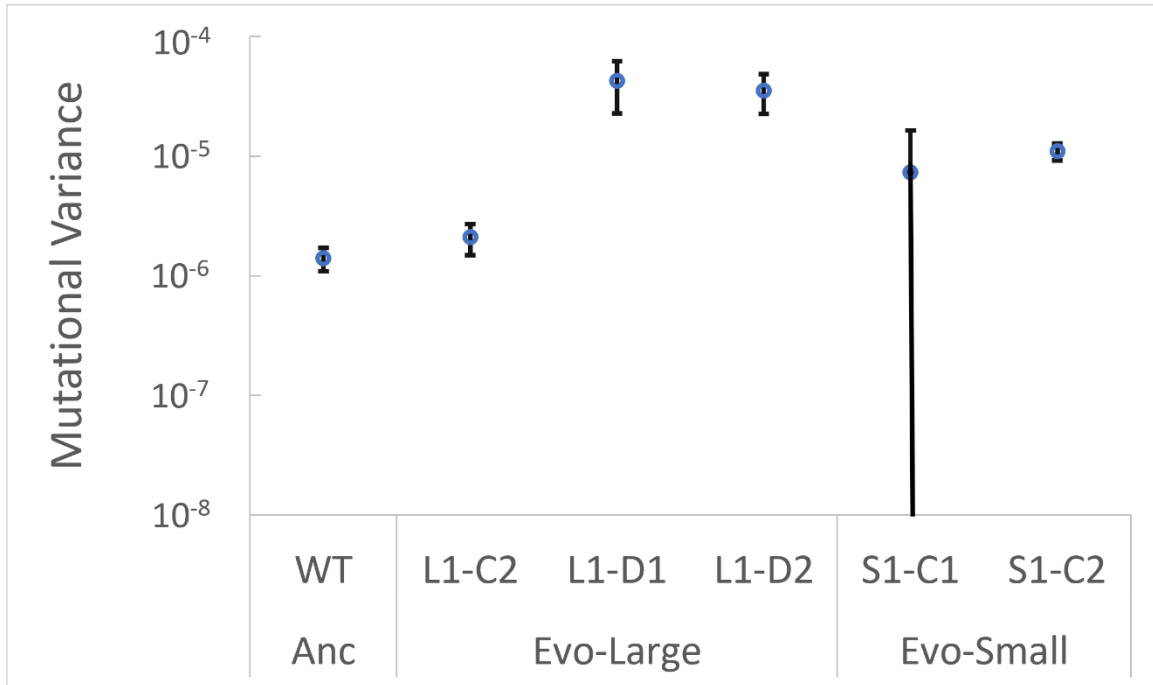


**Figure 1: Comparison of mutational variance of  $\mu_{\max}$  between WT ancestor-derived MA experiments and WT evolved population-derived MA experiments.** The mutational variance is the estimated input of variance per generation attributed to spontaneous mutations. The mutational variance of  $\mu_{\max}$  was calculated for the WT ancestor-derived MA experiment (Anc) and several WT evolved population-derived MA experiments, which are categorized based on the populations' daily transfer sizes (Evo-Large or Evo-Small). The calculated mutational variance values and their associated standard errors are plotted on a logarithmic scale. The lower standard error value of MA experiment S1-C1 is negative and cannot be plotted on a logarithmic scale.

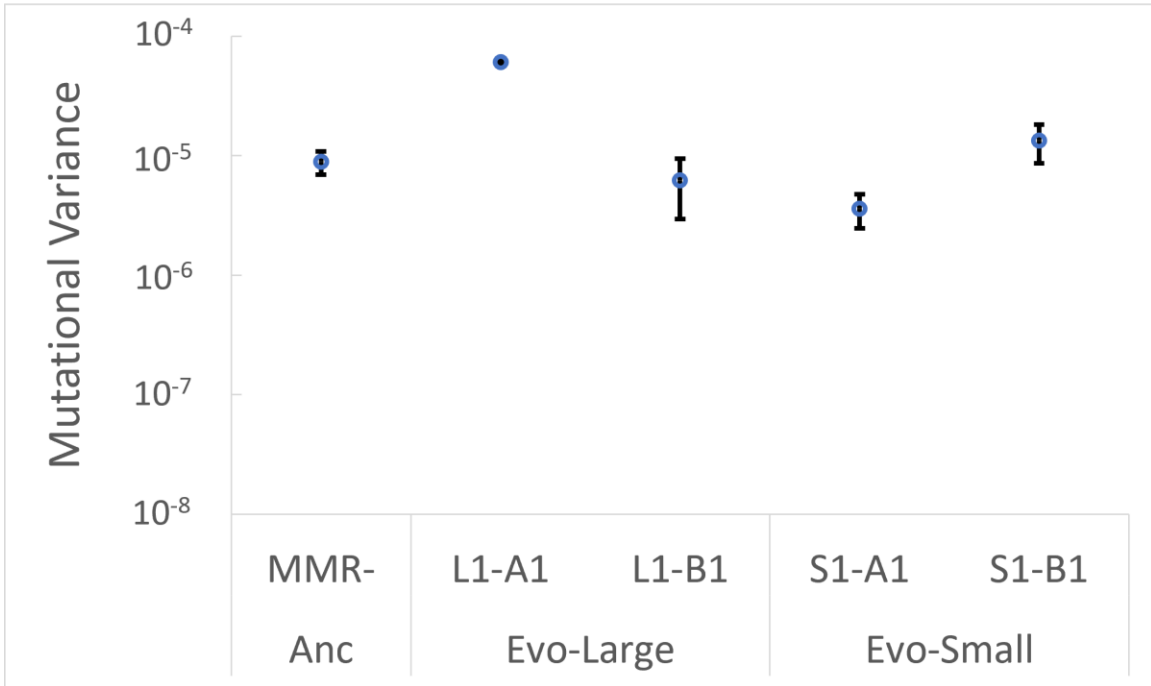


**Figure 2: Comparison of mutational variance of  $\mu_{\max}$  between MMR- ancestor-derived MA experiments and MMR- evolved population-derived MA experiments.** The mutational variance is the estimated input of variance per generation attributed to spontaneous mutations. The mutational variance of  $\mu_{\max}$  was calculated for the MMR- ancestor-derived MA experiment (Anc) and several MMR- evolved population-derived MA experiments, which are categorized based on the populations' daily transfer sizes (Evo-Large or Evo-Small). The calculated mutational variance values and their associated standard errors are plotted on a logarithmic scale.

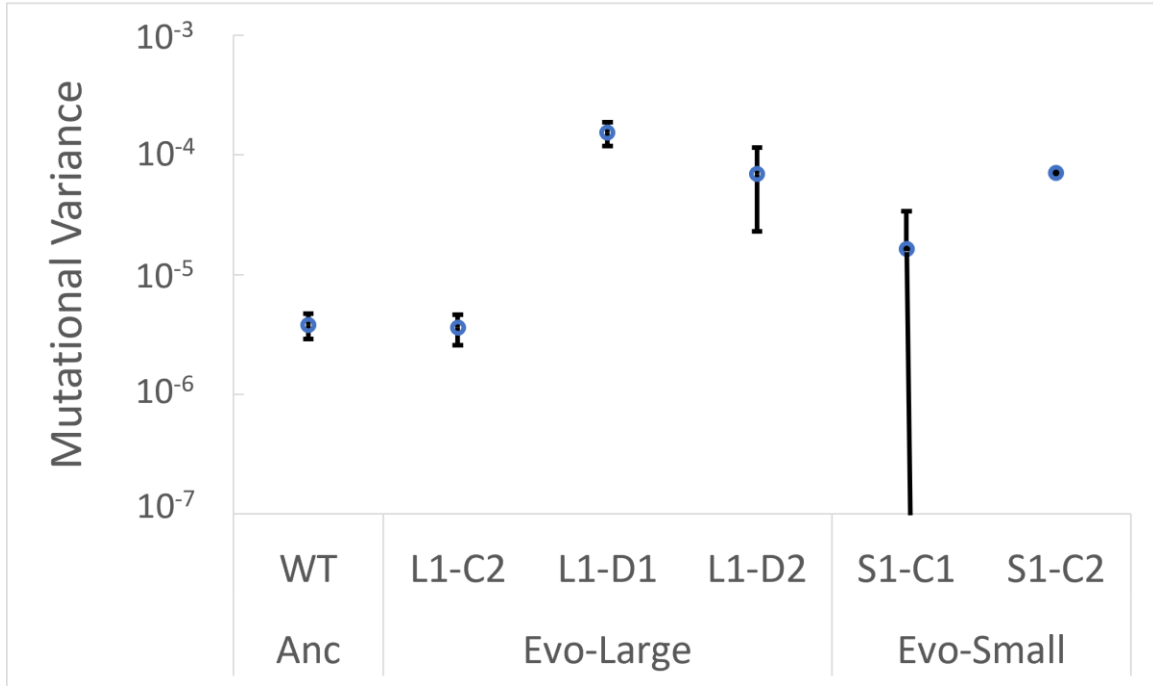


**Figure 3: Comparison of mutational variance of  $K_c$  between WT ancestor-derived MA experiments and WT evolved population-derived MA experiments.** The mutational variance is the estimated input of variance per generation attributed to spontaneous mutations. The mutational variance of  $K_c$  was calculated for the WT ancestor-derived MA experiment (Anc) and several WT evolved population-derived MA experiments, which are categorized based on the populations; daily transfer sizes (Evo-Large or Evo-Small). The calculated mutational variance values and their associated standard errors are plotted on a logarithmic scale. The lower standard error value of MA experiment S1-C1 is negative and cannot be plotted on a logarithmic scale.

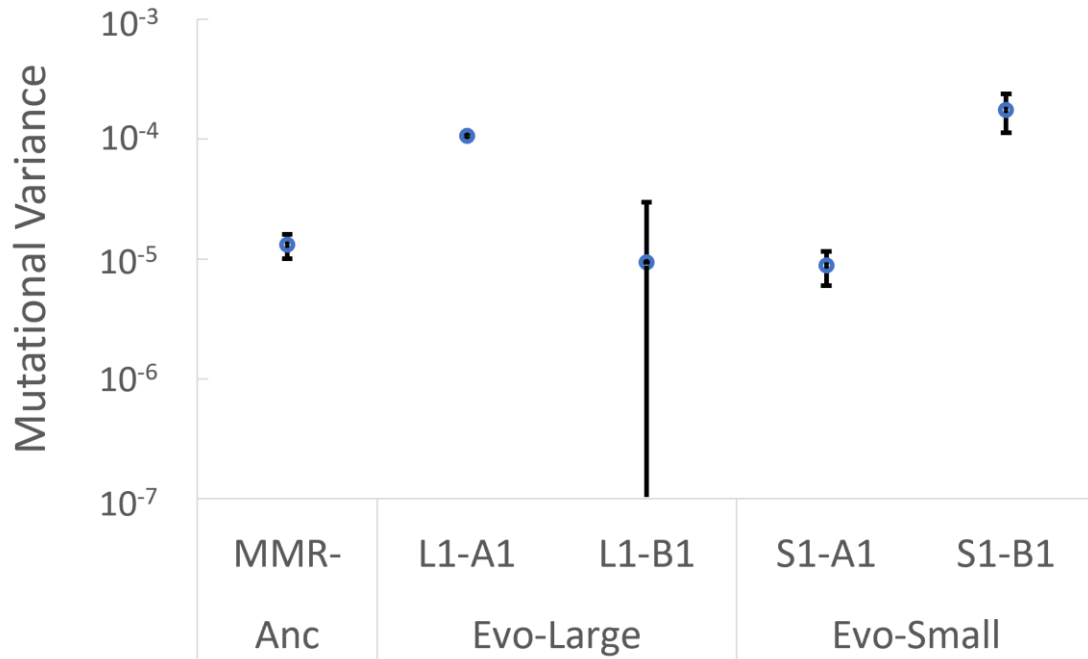


**Figure 4: Comparison of mutational variance of  $K_c$  between MMR- ancestor-derived MA experiments and MMR- evolved population-derived MA experiments.** The mutational variance is the estimated input of variance per generation attributed to spontaneous mutations. The mutational variance of  $K_c$  was calculated for the MMR- ancestor-derived MA experiment (Anc) and several MMR- evolved population-derived MA experiments, which are categorized based on the populations' daily transfer sizes (Evo-Large or Evo-Small). The calculated mutational variance values and their associated standard errors are plotted on a logarithmic scale. The lower standard error value of MA experiment L1-B1 is negative and cannot be plotted on a logarithmic scale.

## Expectation of Mutational Effects

With the observation that  $V_m$  has evolved in several *E. coli* populations during experimental evolution, the next question was to examine whether the observed changes in  $V_m$  could be explained by changes in mutational effect size. Therefore, the expectation of mutational effects,  $E(a)$ , was estimated by the sum of spontaneous mutational effects on a phenotype divided by the total number of spontaneous mutations (Wei, et al. 2022), under the assumption of an additive model of mutational effects.

The  $E(a)$  of the evolved population were compared to the  $E(a)$  of the corresponding ancestor. This comparison would reveal how the mean mutational effect size of the two growth-related traits have evolved from the ancestral state during experimental evolution.

The analysis with  $\mu_{\max}$  shows that two of the five WT evolved population-derived MA experiments display significantly different  $E(a)$  values compared to the WT ancestor-derived MA experiment (**Figure 5**). MA experiment S1-C1 displays a lower  $E(a)$  compared to the ancestral value, while MA experiment S1-C2 displays a higher  $E(a)$  compared to the WT ancestor (**Figure 5**). None of the MMR- evolved population-derived MA experiments show any significant changes in  $E(a)$  compared to the MMR- ancestor-derived MA experiment (**Figure 6**).

Continuing the analysis with the  $K_c$  trait, the same two WT evolved population-derived MA experiments display  $E(a)$  values that are significantly different from the WT ancestor-derived MA experiment (**Figure 7**). The same pattern persists in that the  $E(a)$  of MA experiment S1-C1 is lower than the ancestor, while the  $E(a)$  of MA experiment S1-C2 is higher than the ancestor (**Figure 7**). For the MMR- MA experiments, MA

experiment L1-A1 displays an  $E(a)$  that is significantly higher compared to the MMR-ancestor-derived MA experiment (**Figure 8**).

These results show that two populations – S1-C and L1-A – display a significant change in  $E(a)$  after 1000 days of experimental evolution compared to the day-0 ancestral values, suggesting that the mean mutational effect size has evolved in these populations during experimental evolution. However, most populations show no significant change in  $E(a)$  compared to the ancestor, despite several of them displaying an increase in  $V_m$  after experimental evolution. This discrepancy between the  $V_m$  results and the  $E(a)$  results suggests that the observed changes in  $V_m$  cannot be sufficiently explained by the evolution of mean mutational effect size.

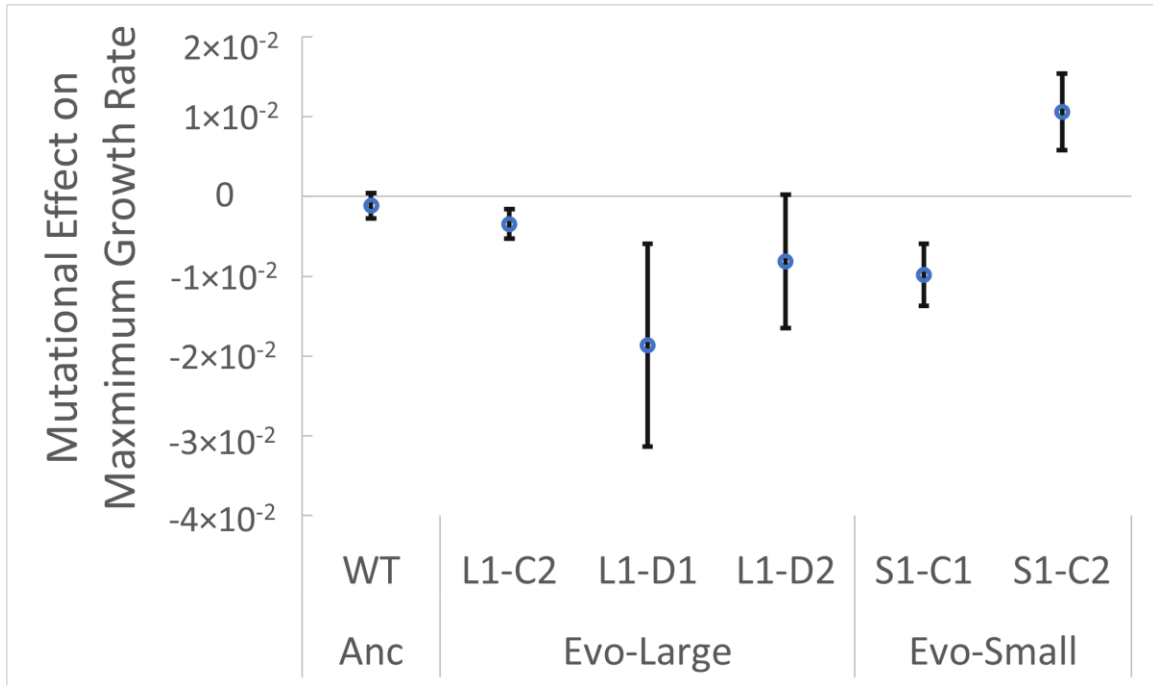


**Figure 5: Expectation of mutational effects on  $\mu_{\max}$  within the WT ancestor and WT evolved populations.** Growth curve data and mutational data from the WT ancestor-derived (Anc) and WT evolved population-derived MA experiments were used to calculate the mutational effects ( $E(a)$ ) on  $\mu_{\max}$  relative to the appropriate MA progenitor. The evolved population-derived MA experiments are categorized based on the populations' daily transfer sizes (Evo-Large or Evo-Small). The line at  $y=0$  denotes the average  $\mu_{\max}$  of each respective MA progenitor. A positive  $y$  value indicates an increase in the maximum growth rate relative to the progenitor, while a negative  $y$  value indicates a decrease.

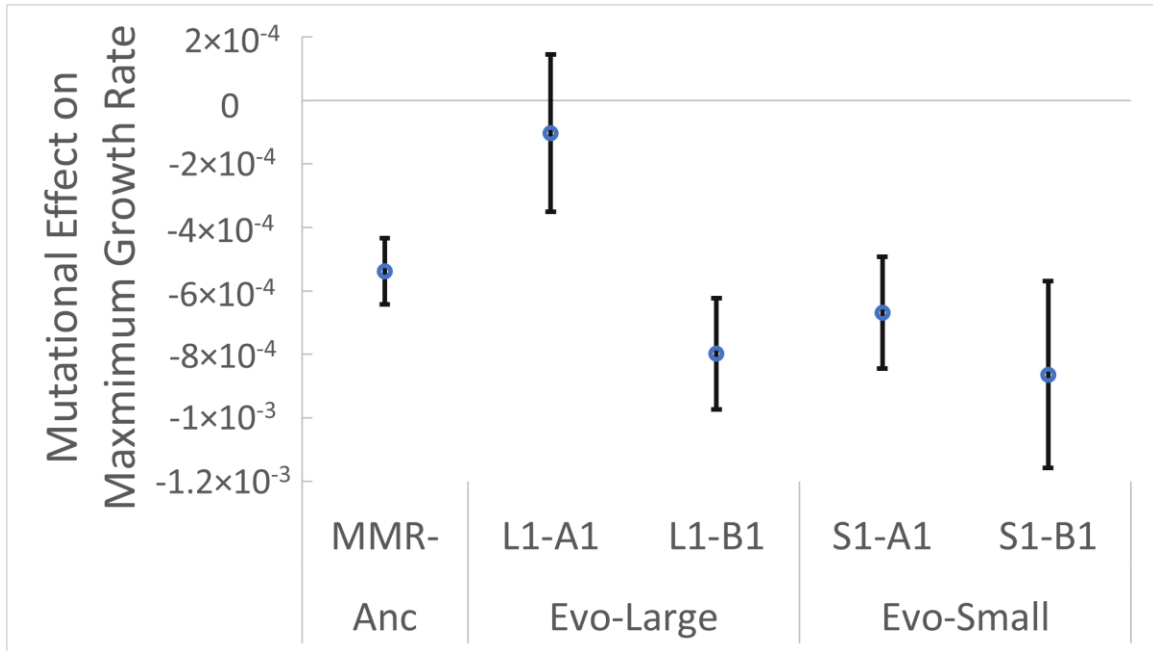


**Figure 6. Expectation of mutational effects on  $\mu_{\max}$  within the MMR- ancestor and MMR-evolved populations.** Growth curve data and mutational data from the MMR- ancestor-derived (Anc) and MMR- evolved population-derived MA experiments were used to calculate the mutational effects ( $E(a)$ ) on  $\mu_{\max}$  relative to the appropriate MA progenitor. The evolved population-derived MA experiments are categorized based on the populations' daily transfer sizes (Evo-Large or Evo-Small). The line at  $y=0$  denotes the average  $\mu_{\max}$  of each respective MA progenitor. A positive  $y$  value indicates an increase in the maximum growth rate relative to the progenitor, while a negative  $y$  value indicates a decrease.

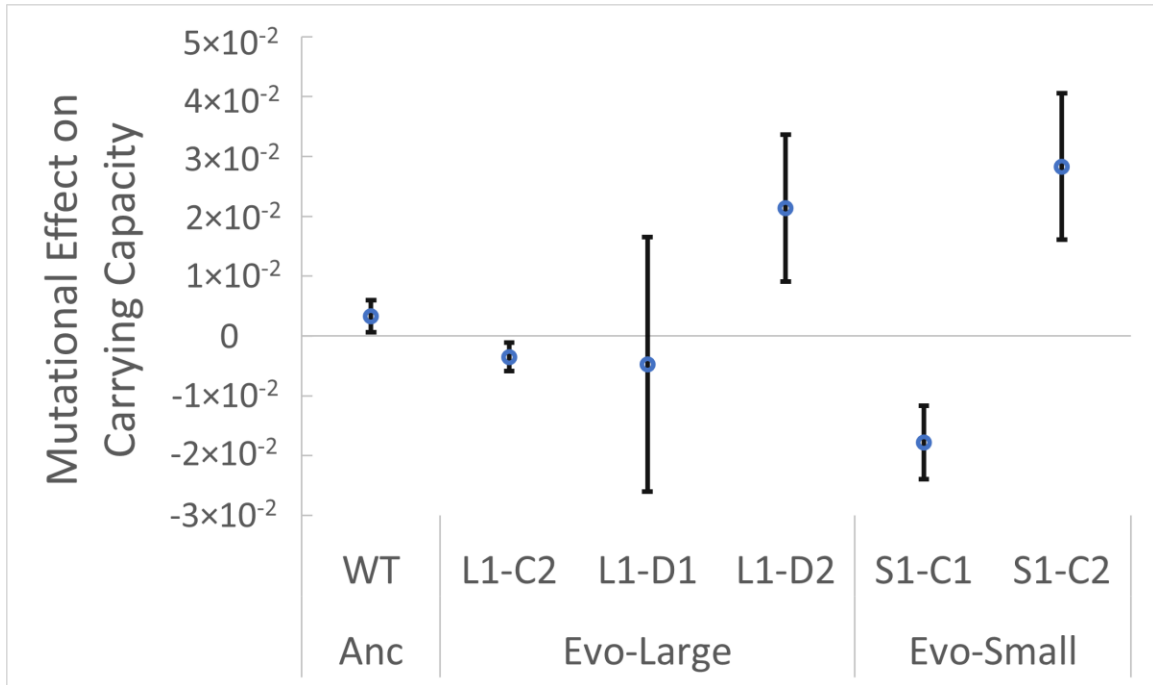


**Figure 7. Expectation of mutational effects on  $K_c$  within the WT ancestor and WT evolved populations.** Growth curve data and mutational data from the WT ancestor-derived (Anc) and WT evolved population-derived MA experiments were used to calculate the mutational effects ( $E(a)$ ) on  $K_c$  relative to the appropriate MA progenitor. The evolved population-derived MA experiments are categorized based on the populations' daily transfer sizes (Evo-Large or Evo-Small). The line at  $y=0$  denotes the average  $K_c$  of each respective MA progenitor. A positive  $y$  value indicates an increase in the carrying capacity relative to the progenitor, while a negative  $y$  value indicates a decrease.

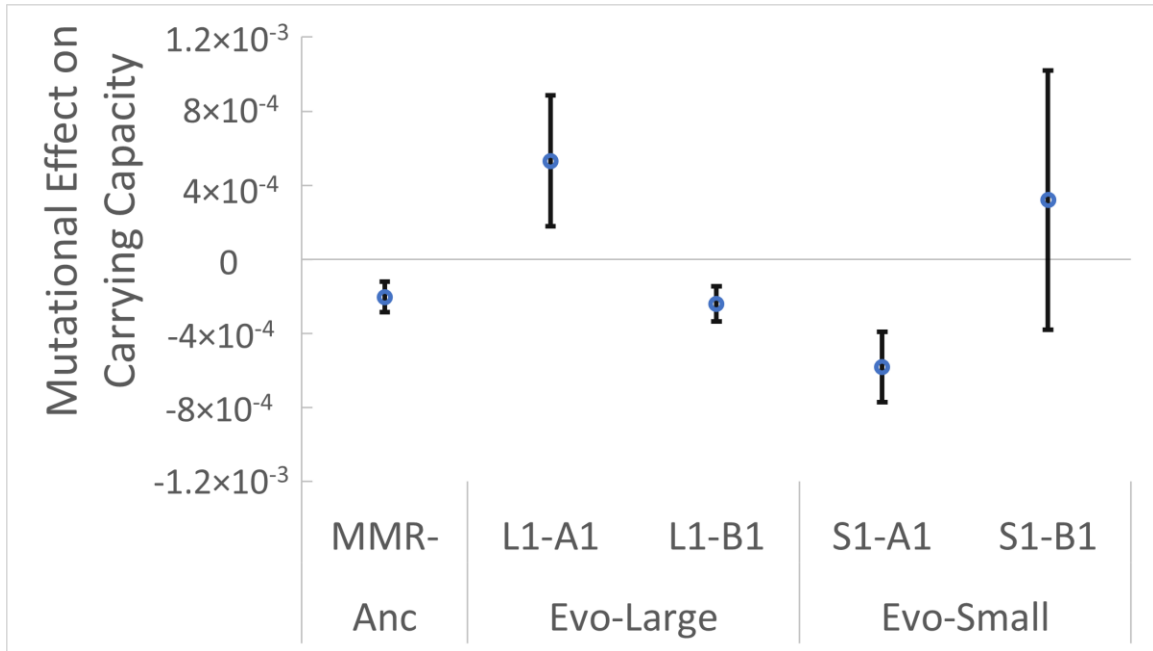


**Figure 8. Expectation of mutational effects on  $K_c$  within the MMR- ancestor and MMR-evolved populations.** Growth curve data and mutational data from the MMR- ancestor-derived (Anc) and MMR- evolved population-derived MA experiments were used to calculate the mutational effects ( $E(a)$ ) on  $K_c$  relative to the appropriate MA progenitor. The evolved population-derived MA experiments are categorized based on the populations' daily transfer sizes (Evo-Large or Evo-Small). The line at  $y=0$  denotes the average  $K_c$  of each respective MA progenitor. A positive  $y$  value indicates an increase in the carrying capacity relative to the progenitor, while a negative  $y$  value indicates a decrease.

## Expectation of Square Mutational Effects

Though the investigation of the evolution of mean mutational effect size did not provide an adequate explanation for the observed changes in  $V_m$ , this study sought to investigate the relationship between mutational effects and  $V_m$  further by considering the effect of mutation rate on the observed  $V_m$  results. According to the mutational data (Wei, et al. 2022), the mutation rates of the *E. coli* populations have evolved from the ancestral state, which has resulted in a noticeable difference in the total number of mutations accumulated during the MA experiments. However, the initial analysis of  $V_m$  did not account for the difference in the number of spontaneous mutations accumulated when comparing the evolved population-derived and ancestor-derived MA experiments. In theory,  $V_m = U \times E(a^2)$  (Lynch and Walsh 1998), where  $U$  is the population's mutation rate and  $E(a^2)$  is the expectation of square mutational effects, or the genetic variance per mutation, assuming an additive model. Thus, the observed changes in  $V_m$  may be attributed to changes in  $U$ ,  $E(a^2)$ , or both. Therefore, the next step in investigating the relationship between mutational effects and  $V_m$  was to study how  $E(a^2)$  has changed during experimental evolution.

Using the  $V_m$  values calculated previously, and the  $U$  values obtained from the mutational data (Wei, et al. 2022),  $E(a^2)$  was calculated for each MA experiment by  $V_m/U$ . The  $E(a^2)$  of the evolved population-derived MA experiments were then compared to the  $E(a^2)$  of the appropriate ancestor-derived MA experiment. This comparison would reveal how the mutational effects on the genetic variance of the two growth-related traits have evolved from the ancestral state during experimental evolution.

The analysis of  $\mu_{\max}$  revealed that three of the five WT evolved population-derived MA experiments – L1-D1, L1-D2, and S1-C2 – display significantly higher  $E(a^2)$  values compared to the WT ancestor-derived MA experiment (**Figure 9**). Of the four MMR- evolved population-derived MA experiments, only MA experiment L1-A1 displays a significantly different  $E(a^2)$  compared to the MMR- ancestor-derived MA experiment (**Figure 10**).

Continuing the analysis with the  $K_c$  trait, two of the five WT evolved population-derived MA experiments – L1-D1 and S1-C2 – show an increase in  $E(a^2)$  compared to the ancestor-derived MA experiment (**Figure 11**). For the MMR- MA experiments, two of the four – L1-A1 and S1-B1 – display a significant increase in  $E(a^2)$  compared to the MMR- ancestor derived MA experiment (**Figure 12**).

These results show that several populations – L1-D, S1-C, L1-A, and S1-B – display a significant increase in  $E(a^2)$  after 1000 days of experimental evolution compared to the day-0 ancestral values, suggesting that the mutational effects on genetic variance have evolved in these populations during experimental evolution. Notably, the MA experiments that showed an increase in  $E(a^2)$  compared to the ancestor are the same MA experiments that displayed an increase in  $V_m$  compared to the ancestor. This suggests that the evolution of mutational effects on genetic variance contributed significantly to, and thus adequately explain, the evolution of  $V_m$  within the *E. coli* populations.

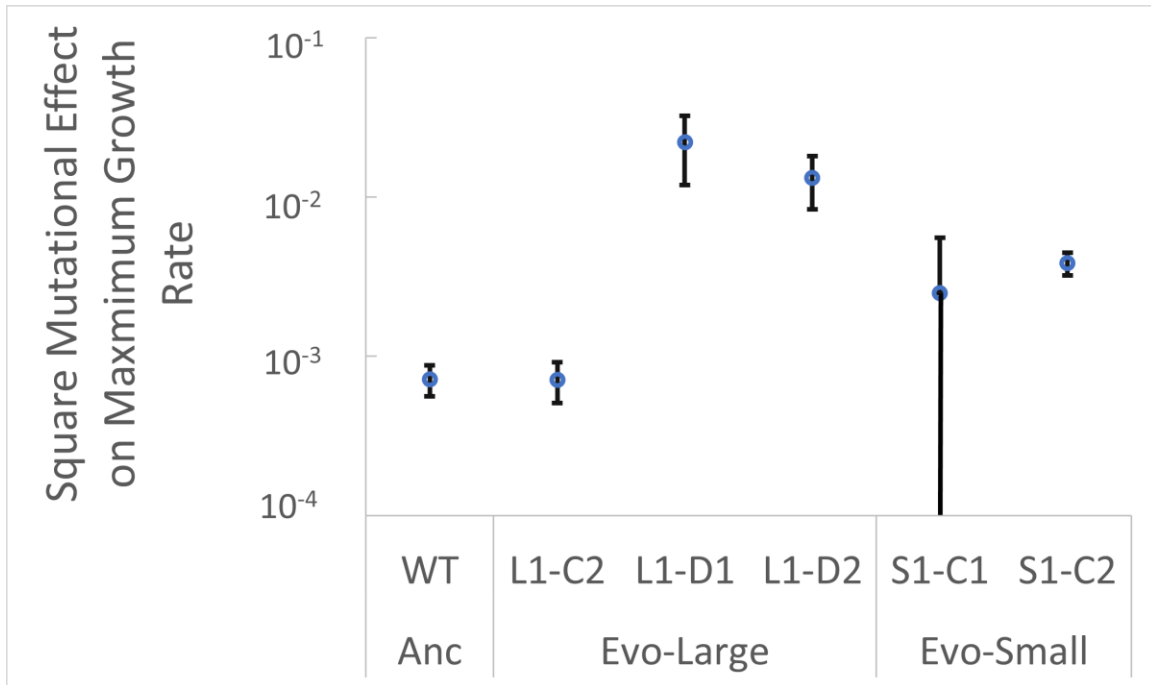


**Figure 9: Expectation of square mutational effects on  $\mu_{\max}$  within the WT ancestor and WT evolved populations.**  $V_m$  data and mutational data from the WT ancestor-derived (Anc) and WT evolved population-derived MA experiments were used to calculate the square mutational effects ( $E(a^2)$ ) on  $\mu_{\max}$  relative to the appropriate MA progenitor. The evolved population-derived MA experiments are categorized based on the populations' daily transfer sizes (Evo-Large or Evo-Small). The calculated  $E(a^2)$  values and their associated standard errors are plotted on a logarithmic scale. The lower standard error value of MA experiment S1-C1 is negative and cannot be plotted on a logarithmic scale.

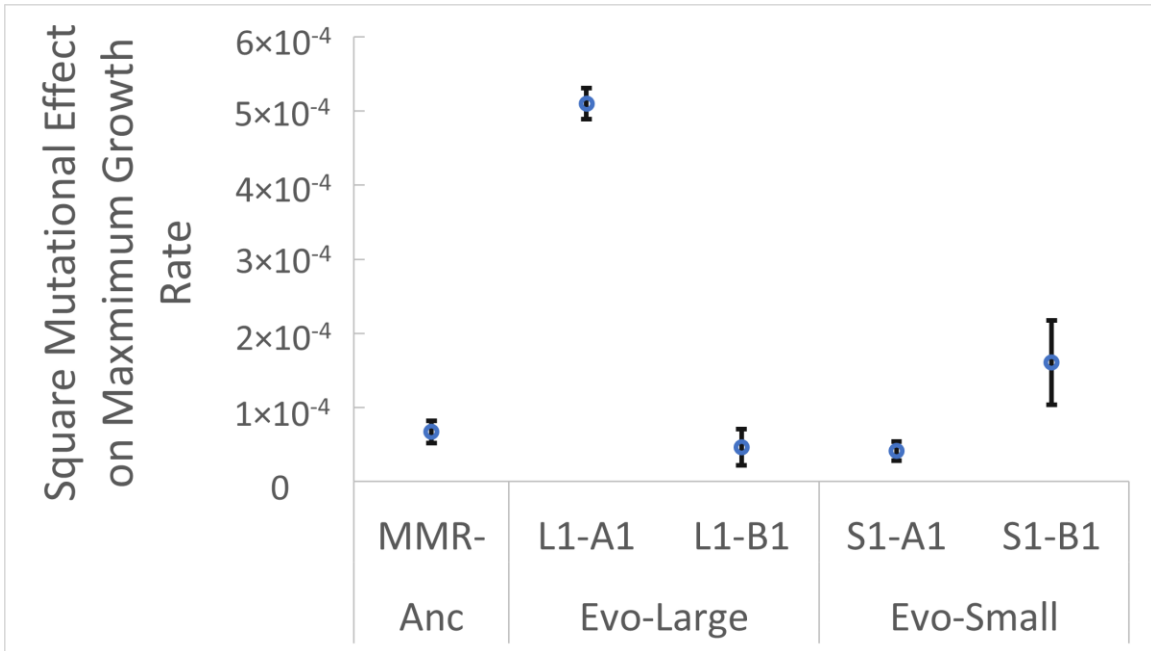


**Figure 10: Expectation of square mutational effects on  $\mu_{\max}$  within the MMR- ancestor and MMR- evolved populations.**  $V_m$  data and mutational data from the MMR- ancestor-derived (Anc) and MMR- evolved population-derived MA experiments were used to calculate the square mutational effects ( $E(a^2)$ ) on  $\mu_{\max}$  relative to the appropriate MA progenitor. The evolved population-derived MA experiments are categorized based on the populations' daily transfer sizes (Evo-Large or Evo-Small).

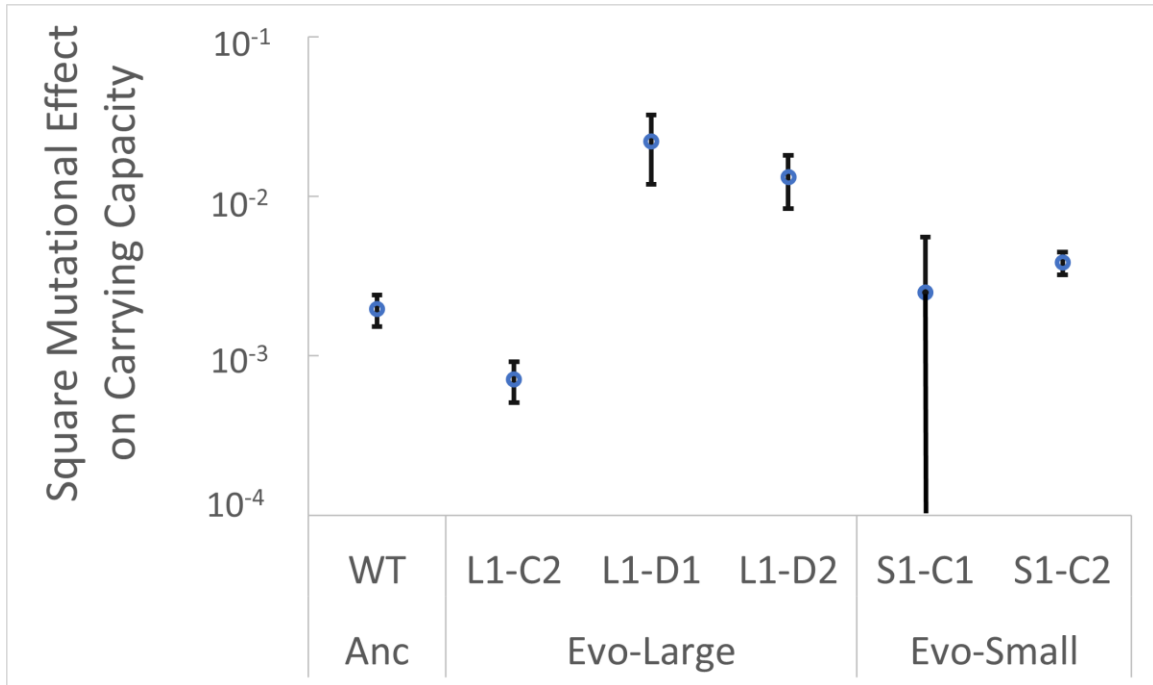


**Figure 11: Expectation of square mutational effects on  $K_c$  within the WT ancestor and WT evolved populations.**  $V_m$  data and mutational data from the WT ancestor-derived (Anc) and WT evolved population-derived MA experiments were used to calculate the square mutational effects ( $E(a^2)$ ) on  $K_c$  relative to the appropriate MA progenitor. The evolved population-derived MA experiments are categorized based on the populations' daily transfer sizes (Evo-Large or Evo-Small). The calculated  $E(a^2)$  values and their associated standard errors are plotted on a logarithmic scale. The lower standard error value of MA experiment S1-C1 is negative and cannot be plotted on a logarithmic scale.

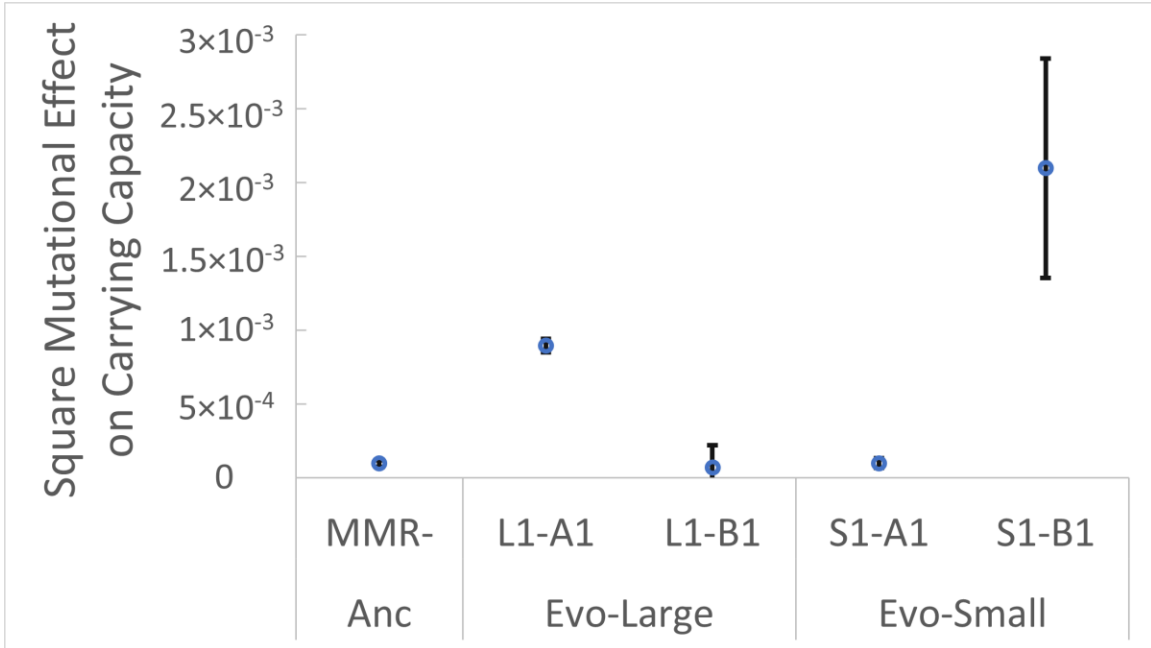


**Figure 12: Expectation of square mutational effects on  $K_c$  within the MMR- ancestor and MMR- evolved populations.**  $V_m$  data and mutational data from the MMR- ancestor-derived (Anc) and MMR- evolved population-derived MA experiments were used to calculate the square mutational effects ( $E(a^2)$ ) on  $K_c$  relative to the appropriate MA progenitor. The evolved population-derived MA experiments are categorized based on the populations' daily transfer sizes (Evo-Large or Evo-Small). The lower standard error value of MA experiment L1-B1 is negative and extends below the minimum value of  $y=0$ .

## Response of Genetic Variance to Experimental Evolution

To understand the mode of phenotypic evolution in growth-related traits, the final goal of this study was to measure the accumulation rate of genetic variance ( $V_{W'}$ ) during experimental evolution and compare the results to the previous  $V_m$  results. As mentioned,  $V_m$  serves as a critical parameter for predicting  $V_{W'}$  in the absence of selection. Thus, a discrepancy between the observed  $V_{W'}$ , which is measured in the presence of selection, and the  $V_m$  expectation may suggest the involvement of selection in the evolution of growth-related traits.

Because  $V_{W'}$  is measured in the presence of selection, the day-1000 evolved *E. coli* populations were utilized for this analysis, as opposed to the derived MA experiments. To calculate  $V_{W'}$ , growth curve data were first collected for each experimentally evolved population. As mentioned previously, each evolved population consists of up to 40 clones, with up to 16 replicates per clone. The growth curve data for the evolved populations were calculated relative to the appropriate day-0 ancestor. After collecting the growth curve data, an ANOVA was used to partition the different portions of variances of the  $\mu_{\max}$  and  $K_c$  traits, including the within population component ( $V_W$ ) and the residual environmental component ( $V_E$ ) for each population. Using  $V_W$  and the total generation number in the experimental evolution ( $g$ ),  $V_{W'}$  was estimated by  $V_W/g$  for each population.

The  $V_{W'}$  of each evolved population was then compared to the  $V_m$  of the MA experiment(s) derived from that population. This comparison would reveal whether the growth-related traits show evidence of selection, and which mode of selection the changes in variance most closely resemble.

Beginning the analysis with the  $\mu_{\max}$  trait, all three of the WT evolved populations – L1-C, L1-D, and S1-C – demonstrate a significantly lower  $V_{W'}$  (**Figure 13**) compared to the  $V_m$  of the evolved population-derived MA experiment (**Figure 1**). However, for populations L1-D and L1-C, both of which have two derived MA experiments available for comparison, the  $V_{W'}$  of the evolved population (**Figure 13**) is only lower than the  $V_m$  of one derived MA experiment, and not significantly different from the  $V_m$  of the other, leading to inconclusive results (**Figure 1**). For the MMR- evolved populations, three of the four populations – L1-A, S1-A, and S1-B – display a significantly lower  $V_{W'}$  (**Figure 14**) compared to the  $V_m$  of the respective derived MA experiment (**Figure 2**). MMR- population L1-B uniquely shows a significantly higher  $V_{W'}$  (**Figure 14**) compared to its derived MA experiment (**Figure 2**).

Continuing the analysis with the  $K_c$  trait, the three WT evolved populations again demonstrate significantly lower  $V_{W'}$  values (**Figure 15**) compared to the  $V_m$  expectation of the derived MA experiment (**Figure 3**). However, for populations L1-D and S1-C, the results are still inconclusive as the populations  $V_{W'}$  values (**Figure 15**) are only lower than the  $V_m$  of one of the two derived MA experiments (**Figure 3**). For the MMR- populations, three of the four populations – L1-A, S1-A, and S1-B – demonstrate a lower  $V_{W'}$  (**Figure 16**) compared to the  $V_m$  of the derived MA experiment (**Figure 4**).

The results show that several evolved *E. coli* populations display  $V_{W'}$  values that are significantly lower than the  $V_m$  expectations of their respective derived MA experiments. This suggests that selection has influenced the phenotypic outcomes of these growth-related traits during experimental evolution. Specifically, the influence of selection has resulted in a lower genetic variance than would be expected in the absence

of selection for most of these populations. A notable exception is the MMR- evolved population L1-B, which has evolved a higher-than-expected genetic variance in the presence of selection. Additionally WT evolved populations L1-D and S1-C demonstrate inconsistent results when comparing the  $V_w'$  of these populations to the  $V_m$  of the two derived MA experiments. Thus, a firm conclusion cannot be made regarding the influence of selection on these two populations.

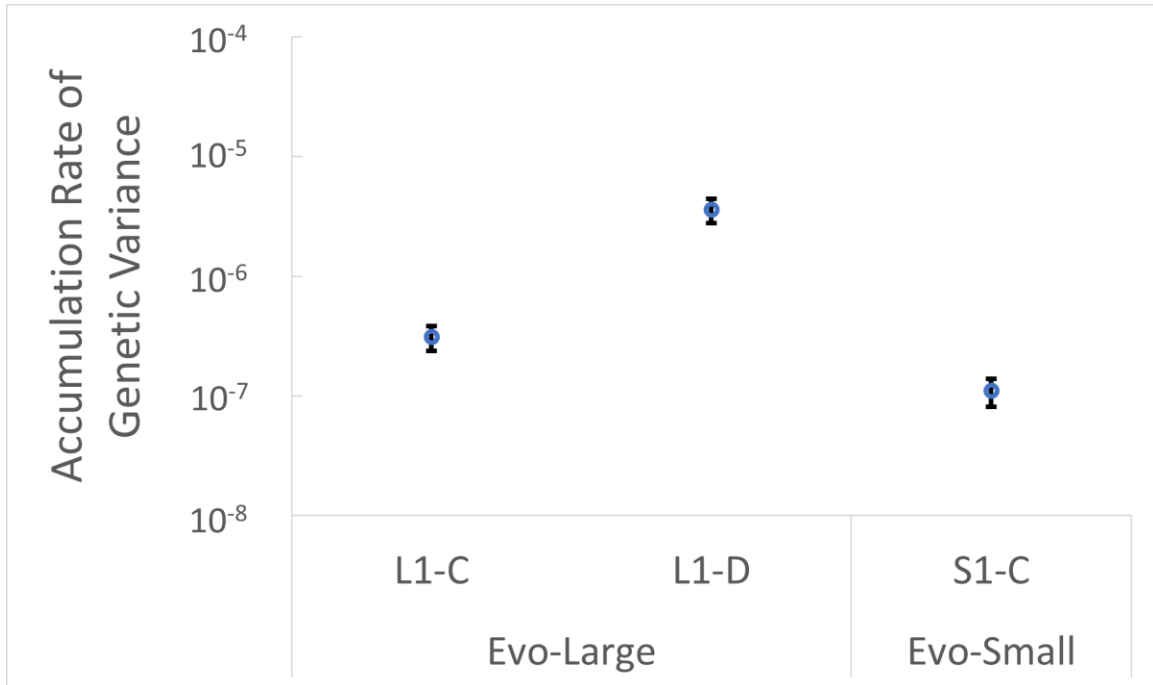


**Figure 13: Accumulation rate of genetic variance of  $\mu_{\max}$  among WT evolved populations.** The accumulation rate of genetic variance is the input of within-population variance per generation calculated for each experimentally evolved population. The accumulation rate of genetic variance of  $\mu_{\max}$  was calculated for the WT evolved populations, which are categorized based on their daily transfer size (Evo-Large or Evo-Small). The calculated accumulation rates and their associated standard errors are plotted on a logarithmic scale.

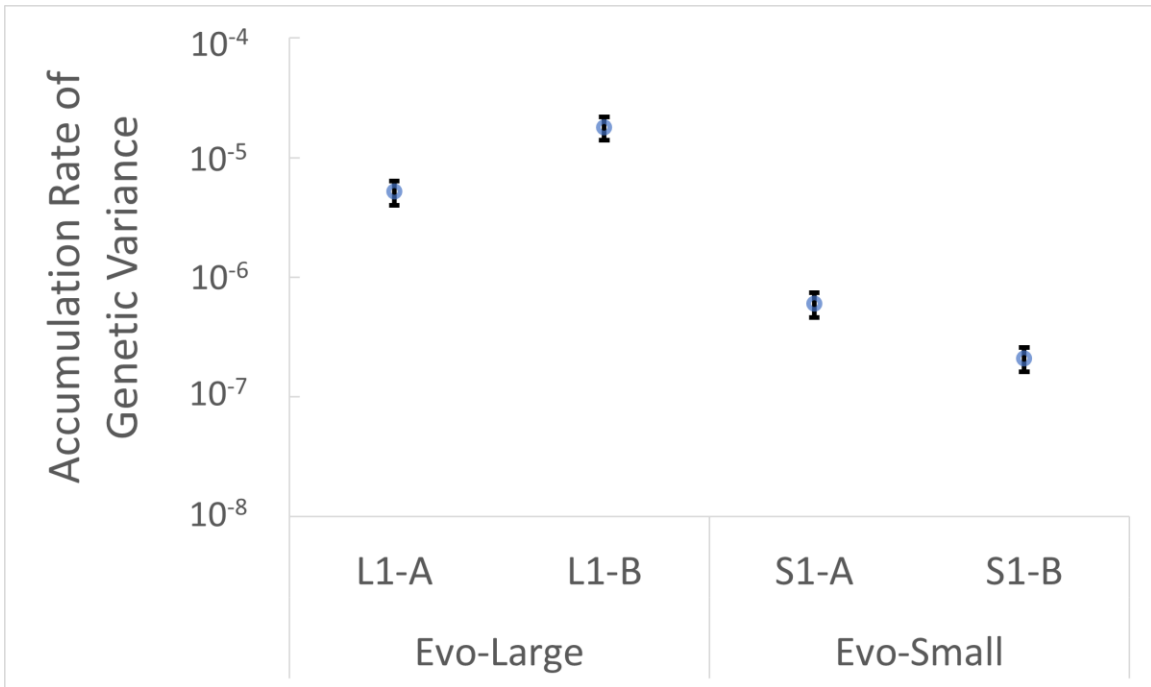


**Figure 14: Accumulation rate of genetic variance of  $\mu_{\max}$  among MMR- evolved populations.** The accumulation rate of genetic variance is the input of within-population variance per generation calculated for each experimentally evolved population. The accumulation rate of genetic variance of  $\mu_{\max}$  was calculated for the MMR- evolved populations, which are categorized based on their daily transfer size (Evo-Large or Evo-Small). The calculated accumulation rates and their associated standard errors are plotted on a logarithmic scale.

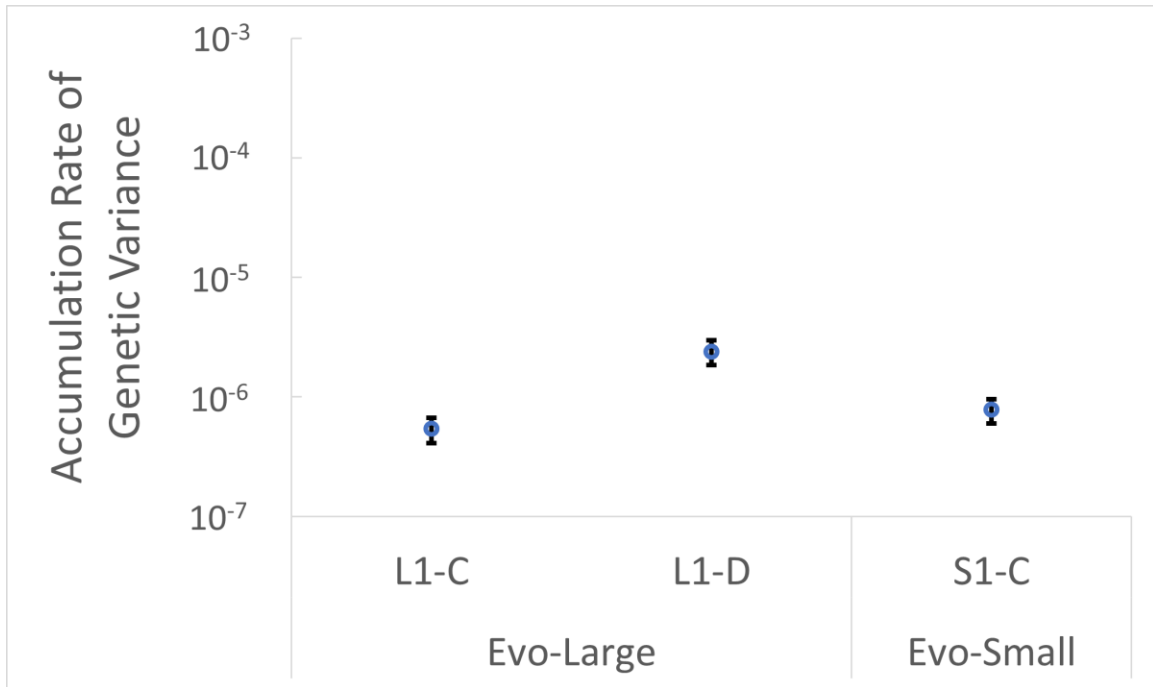


**Figure 15: Accumulation rate of genetic variance of  $K_c$  among WT evolved populations.** The accumulation rate of genetic variance is the input of within-population variance per generation calculated for each experimentally evolved population. The accumulation rate of genetic variance of  $K_c$  was calculated for the WT evolved populations, which are categorized based on their daily transfer size (Evo-Large or Evo-Small). The calculated accumulation rates and their associated standard errors are plotted on a logarithmic scale.

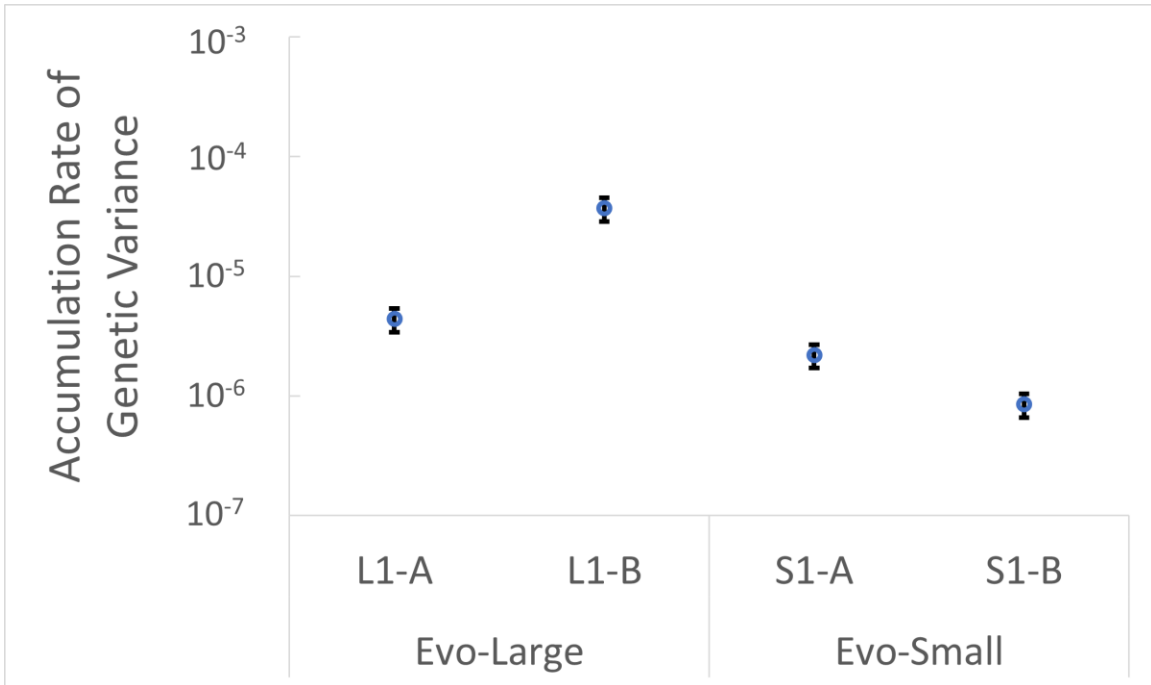


**Figure 16: Accumulation rate of genetic variance of  $K_c$  among MMR- evolved populations.** The accumulation rate of genetic variance is the input of within-population variance per generation calculated for each experimentally evolved population. The accumulation rate of genetic variance of  $K_c$  was calculated for the MMR- evolved populations, which are categorized based on their daily transfer size (Evo-Large or Evo-Small). The calculated accumulation rates and their associated standard errors are plotted on a logarithmic scale.

## **Discussion**

### **Evolution of Mutational Variance During Experimental Evolution**

The first step in investigating the evolution of mutational and phenotypic outcomes in the experimentally evolved *E. coli* populations was to measure the  $V_m$  of the  $\mu_{\max}$  and  $K_c$  traits within these populations.  $V_m$  was a vital component of this study, as it represents the change of genetic variance attributed to spontaneous mutations. Thus, measuring the  $V_m$  within a population allows for the prediction of the expected  $V_W'$  of that population in the absence of selection. This study also sought to determine whether  $V_m$  itself had changed from the ancestral state during experimental evolution. To this end, MA growth curve data was used to measure the  $V_m$  of the day-0 experimental evolution ancestors and the day-1000 evolved populations.

A comparison of the  $V_m$  between the two timepoints revealed that several populations had evolved a higher  $V_m$  compared to the ancestor. The results indicate that the  $V_m$  is indeed subject to change, particularly favoring an excess of variance compared to the ancestor. Furthermore, this increase in  $V_m$  was observed in populations of both genetic backgrounds – WT and MMR- – and both transfer sizes – Large and Small. Therefore, there was not enough evidence to conclude that genetic background and  $N_e$  influence the evolution of  $V_m$ .

### **Expectation of Mutational Effects**

After verifying that the  $V_m$  within several populations had increased from the ancestral value during experimental evolution, the next step was to determine whether these increases in  $V_m$  could be adequately explained by an increase in mutational effect

size. To accomplish this, the  $E(a)$  was estimated for the ancestors and the evolved populations using the previous MA growth curve data, and previously calculated mutational data (Wei, et al. 2022). A comparison between the two timepoints revealed that only two total populations demonstrated a change in mutational effect size from the ancestral state. Additionally, the results of one of these populations, population S1-C, are inconclusive, as its derived MA results indicate that the  $E(a)$  has simultaneously increased and decreased from the ancestral state. Therefore, there was not enough evidence to conclude that the mutational effect size has changed overall within these populations. Thus, the evolution of mutational effect size does not explain the observed changes in  $V_m$ .

### **Expectation of Square Mutational Effects**

Despite the inconclusive results regarding the evolution of mutational effect size, this study sought to investigate the relationship between mutational effects and  $V_m$  further by calculating the change in genetic variance per mutation through  $E(a^2)$ . This analysis would allow for the consideration of the difference in mutation rate, and the resulting difference in the total number of spontaneous mutations, between the ancestors and the evolved populations. As with  $E(a)$ ,  $E(a^2)$  was calculated for the ancestors and the evolved populations, and the results were compared between the two timepoints to reveal how  $E(a^2)$  has changed during experimental evolution. The results of the comparison showed that the genetic variance per mutation has increased in several evolved populations compared to the ancestral state. The populations demonstrating these changes are the same populations that had previously demonstrated an increase in  $V_m$ . These results

suggest that the evolution of mutational effects on genetic variance was a contributing factor in evolution of  $V_m$ , and thus adequately explain the observed changes in  $V_m$ .

### **Response of Genetic Variance to Experimental Evolution**

After analyzing the  $V_m$  results and providing an explanation for the changes observed, the final goal was to analyze the  $V_{W'}$  within the evolved *E. coli* populations and compare the results to the calculated  $V_m$ . Because  $V_m$  serves as the expectation of  $V_{W'}$  in the absence of selection, a discrepancy between the  $V_m$  and  $V_{W'}$  results would indicate that selection has influenced the evolution of  $V_{W'}$ . Populational growth curve data was used to measure the  $V_{W'}$  of the  $\mu_{\max}$  and  $K_c$  traits within each population. These  $V_{W'}$  results were then compared to the previous  $V_m$  expectations to identify significant differences between the two.

The results of the comparison revealed that several populations have evolved a  $V_{W'}$  that is lower than would be expected in the absence of selection, suggesting that selection has influenced the evolution of  $V_{W'}$  in these populations. To be more specific, the observed deficit of genetic variance suggests the involvement of either stabilizing or directional selection, assuming that these populations have reached equilibrium after 1000 days of experimental evolution. However, an analysis of the mean trait values would be necessary to determine which mode of selection is most appropriate. Interestingly, MMR- population L1-B was the one notable exception among these evolved populations in that the  $V_{W'}$  of  $\mu_{\max}$  was higher than the  $V_m$  expectation, suggesting the involvement of disruptive selection under the assumption that the population has reached equilibrium.

The results of the comparison between  $V_{W'}$  and  $V_m$  demonstrated no clear trend regarding the genetic background and transfer size. Therefore, there is not enough evidence to conclude that the genetic background and  $N_e$  have influenced the evolutionary outcomes of the  $\mu_{\max}$  and  $K_c$  traits within the evolved populations.

## **Limitations**

One limitation of this experiment is the sample size of experimentally evolved populations. Due to the quality control cutoffs implemented during the statistical analysis of growth curve data, only seven evolved populations were utilized, resulting in an uneven distribution between the WT (three populations) and MMR- (four populations) backgrounds. The MA experiments derived from these evolved populations were similarly impacted by the cutoffs. For this analysis, only MA experiments derived from the evolved populations that passed quality control were included. As such, this study was restricted to a total of 14 potential MA experiments – two isolates from each population. This was further reduced to nine MA experiments that passed quality control, with only two pairs of isolates that were derived from the same evolved population. Furthermore, performing mutation-accumulation experiments is a time-consuming process. As such, attempting to replace the isolates that did not pass quality control was not feasible. Future studies may benefit from a larger sample of populations and clones/isolates derived from those populations, and potentially an adjustment of quality control parameters that would result in a larger sample size without sacrificing the quality of the data.

Another limitation was the method of calculating the two growth-related trait values that were the focus of this study:  $\mu_{\max}$  and  $K_c$ . As described in Methods, a moving regression was used to evaluate four data points at a time – a timeframe of one hour – and calculate the slope of each of these four points. The slopes of these datapoints were used to find the  $\mu_{\max}$  and  $K_c$  of each growth curve. The moving regression method was chosen as it was simpler and more robust compared to other methods that were tested, such as maximum likelihood fitting to modified Gompertz curves. The moving regression method also allowed for a noticeable expansion of the sample size as it bypassed the need to implement an additional cutoff for log-likelihood. However, the moving regression method involves an arbitrary selection of data points for which the slope is calculated. An increase or decrease in the number of data points evaluated at a time could significantly alter the results of the analysis. Additionally, this method of calculating  $K_c$  has shown to be less effective in cases in which the data points during the stationary phase continue to increase slightly, or in cases of diauxic growth. For future studies, it may be necessary to refine this method in a way that provides more consistent, and less arbitrary, results, or to propose a more effective method of calculating these growth-related traits.

Finally, because this study only utilized two timepoints across the 1000-day experimental evolution – the day-0 start point and the day-1000 endpoint – the interpretations of the results are limited. The conclusions in this study were drawn under the assumption of a linear evolutionary model. This model assumes, for example, that the increase in  $V_m$  observed at the day-1000 timepoint is the result of incremental increases in  $V_m$  from the ancestral state across the entire 1000-day period. However, another possibility is that the  $V_m$  increased sharply towards the end of the 1000-day period. It is

impossible to tell which interpretation is more accurate without analyzing additional intermediate timepoints.

### **Future Studies**

Future studies may expand upon these findings in a number of ways. A similarly designed study that increases the population sample size could better explore the potential relationships between the groupings based on the populations' ancestors and transfer sizes and the evolution of mutational variance and genetic variance within those populations. Moreover, this study's approach only focused on two timepoints: day-0 and day-1000, which may limit the identification of potentially more complicated evolutionary dynamics during the long period of experimental evolution. Therefore, future studies may choose to explore the evolution of variance across additional intermediate time points and evaluate whether the evolutionary trajectories remain consistent or reveal a more complex pattern. Finally, though this study has described the apparent modes of selection expressed by each experimentally evolved population, future studies could explore the environmental source of selection experienced by these populations to provide more context regarding their evolutionary trajectories. These studies might explore the various elements of the growth environment within the experimental design, such as the nutrients within the LB media, and how they could have contributed to the observed evolutionary outcomes.

## Methods

### Populations

This experiment utilized a total of seven experimentally evolved *E. coli* populations that have undergone 1000 days of daily dilutions (Ho, et al. 2021; Wei, et al. 2022). These populations have been split into four treatment groups based on the genetic background and the dilution factor used during this 1000-day cycle. The populations' genetic backgrounds are categorized based on the ancestor from which each population is derived: WT or MMR-. The MMR- ancestor experienced a knockout of the MutL gene, a vital component of the mismatch repair system, which has resulted in a higher mutation rate compared to the WT ancestor that has not experienced the MutL knockout. The populations were further categorized based on their daily transfer size. The “Small” transfer size populations were transferred daily with a dilution factor of  $10^{-7}$ , resulting in a relatively small  $N_e$ . The “Large” transfer size populations were put through a less severe bottleneck with a dilution factor of  $10^{-1}$ , resulting in a relatively large  $N_e$ . Up to 40 clones from each population were collected for this experiment.

This study also utilized nine total MA experiments derived from colonies isolated from the 1000-day experimentally evolved *E. coli* populations (Wei, et al. 2022). After day-1000 of experimental evolution, up to two clones were selected from each of the seven experimentally evolved populations, with each clone serving as a progenitor for a distinct MA experiment. The MA experiments involved 60 days of daily transfers of a single, random colony, beginning with the appropriate day-1000 evolved population progenitor. Up to 24 replicate MA lines were collected for each MA experiment, excluding MA lines with lower-quality sequencing data.

In addition to the evolved population-derived MA experiments, this study utilized MA experiments derived from both the day-0 WT and MMR- ancestors, isolated prior to experimental evolution. The ancestral isolates underwent the same 60-day MA experiment, and up to 42 replicate MA lines were collected from each of the two MA experiments.

### **Growth Curves**

The methods for growth curve data collection involved a 3-step process that included revival of the evolved population clones/MA lines, inoculation, and plate reading. Four clones/MA lines of a single population/MA experiment would be chosen at a time, along with the appropriate control for observing changes in fitness. The control for the day-1000 evolved populations was the day-0 WT or MMR- ancestor, depending on the background of the evolved population, to evaluate the changes that occurred over the course of the 1000-day experimental evolution. The control used for the MA experiments was either the day-0 ancestral progenitor or the day-1000 evolved population progenitor, depending on the MA experiment, to evaluate the changes that occurred over the course of the 60-day MA treatment.

The four clones/MA lines and control were obtained from preserved stock solutions (frozen at  $-80^{\circ}\text{C}$ ) and streaked onto individual TA agar plates. These plates were then incubated at  $37^{\circ}\text{C}$  for a day. After incubating, a single colony from each plate was inoculated in an individual 10mL tube containing 1mL LB. The tubes were incubated at  $37^{\circ}\text{C}$  for another day. After this incubation period, the five tubes of 1mL LB media were each diluted by an additional 9mL LB for a total volume of 10mL. The tubes were

then vortexed to allow for random sampling, and the samples were transferred to a 96-well plate according to the following layout: (1) all wells contain 150 $\mu$ L LB (14,400 $\mu$ L total); (2) column 1 contains no bacteria; (3) columns 2, 7, and 12 contain 15 $\mu$ L of the control (24 wells, 360 $\mu$ L total); (4) columns 3 and 11 contain 15 $\mu$ L of clone/MA line 1 (16 wells, 240 $\mu$ L total); (5) columns 4 and 10 contain 15 $\mu$ L of clone/MA line 2 (16 wells, 240 $\mu$ L total); (6) columns 5 and 9 contain 15 $\mu$ L of clone/MA line 3 (16 wells, 240 $\mu$ L total); and (7) columns 6 and 8 contain 15 $\mu$ L of clone/MA line 4 (16 wells, 240 $\mu$ L total). The lid was then placed on the plate and the seam was sealed with parafilm to minimize evaporation and potential contamination. The plate was placed in a plate reader to read the optical density (OD) over a span of 14 hours. After the read was complete, the data were collected for analysis.

### **Statistical Analysis**

A custom code was used to analyze the data collected from the 96-well plates and estimate growth-related trait values for each replicate (well). The method used to evaluate the growth curves was a moving regression that evaluated four contiguous data points at a time – a timeframe of one hour – and calculated the slope for each grouping. The highest slope among the groupings within the first 10 hours was determined to be  $\mu_{\max}$ .  $K_c$  was derived from the OD of the first grouping after the  $\mu_{\max}$  timepoint with a slope of 0. A sample size cutoff was implemented to exclude clones/MA lines in which growth-related trait values could not be calculated. The average growth-related trait values for each clone/MA line were calculated and plotted relative to the appropriate control, with the

average control value being equal to 1. Particular lines that showed extreme trait values were rerun to verify the results.

## REFERENCES

- Aubin-Horth, Nadia, and Susan C.P. Renn. "Genomic reaction norms: using integrative biology to understand molecular mechanisms of phenotypic plasticity." *Molecular ecology* 18.18 (2009): 3763-3780.
- Barton, Nicholas H., Alison M. Etheridge, and Amandine Véber. "The infinitesimal model: Definition, derivation, and implications." *Theoretical population biology* 118 (2017): 50-73.
- Bataillon, Thomas, and Susan F. Bailey. "Effects of new mutations on fitness: insights from models and data." *Annals of the New York Academy of Sciences* 1320.1 (2014): 76-92.
- Eyre-Walker, Adam, and Peter D. Keightley. "The distribution of fitness effects of new mutations." *Nature Reviews Genetics* 8.8 (2007): 610-618.
- Fisher, Ronald A. "XV.—The correlation between relatives on the supposition of Mendelian inheritance." *Earth and Environmental Science Transactions of the Royal Society of Edinburgh* 52.2 (1918): 399-433.
- Ho, Wei-Chin, et al. "Evolutionary dynamics of asexual hypermutators adapting to a novel environment." *Genome biology and evolution* 13.12 (2021): evab257.
- Kimura, Motoo. "The neutral theory of molecular evolution." *Scientific American* 241.5 (1979): 98-129.
- Kimura, Motoo. "The neutral theory of molecular evolution: a review of recent evidence." *The Japanese Journal of Genetics* 66.4 (1991): 367-386.
- Lande, Russell. "Natural selection and random genetic drift in phenotypic evolution." *Evolution* (1976): 314-334.
- Loewe, Laurence, and William G. Hill. "The population genetics of mutations: good, bad and indifferent." *Philosophical Transactions of the Royal Society B: Biological Sciences* 365.1544 (2010): 1153-1167.
- Lynch, Michael, and Bruce Walsh. *Genetics and analysis of quantitative traits*. Vol. 1. Sunderland, MA: Sinauer, 1998.
- Lynch, Michael, and William G. Hill. "Phenotypic evolution by neutral mutation." *Evolution* 40.5 (1986): 915-935.
- Mackay, T. F. "The genetic architecture of quantitative traits." (2001): 303-339.

- McGuigan, Katrina. "Studying phenotypic evolution using multivariate quantitative genetics." *Molecular ecology* 15.4 (2006): 883-896.
- Neher, Richard A., and Boris I. Shraiman. "Statistical genetics and evolution of quantitative traits." *Reviews of Modern Physics* 83.4 (2011): 1283.
- Ohta, Tomoko. "The nearly neutral theory of molecular evolution." *Annual review of ecology and systematics* (1992): 263-286.
- Orr, H. Allen. "The population genetics of adaptation: the distribution of factors fixed during adaptive evolution." *Evolution* 52.4 (1998): 935-949.
- Pigliucci, Massimo. *Phenotypic plasticity: beyond nature and nurture*. JHU Press, 2001.
- Pigliucci, Massimo. "Evolution of phenotypic plasticity: where are we going now?." *Trends in ecology & evolution* 20.9 (2005): 481-486.
- Scheiner, Samuel M. "Genetics and evolution of phenotypic plasticity." *Annual review of ecology and systematics* (1993): 35-68.
- Stern, David L., and Virginie Orgogozo. "Is genetic evolution predictable?." *Science* 323.5915 (2009): 746-751.
- Stern, David L., and Virginie Orgogozo. "The loci of evolution: how predictable is genetic evolution?." *Evolution: International Journal of Organic Evolution* 62.9 (2008): 2155-2177.
- Wei, Wen, et al. "Rapid evolution of mutation rate and spectrum in response to environmental and population-genetic challenges." *Nature communications* 13.1 (2022): 1-10.
- West-Eberhard, Mary Jane. "Phenotypic plasticity and the origins of diversity." *Annual review of Ecology and Systematics* (1989): 249-278.
- Wray, Gregory A. "Genomics and the evolution of phenotypic traits." *Annual review of ecology, evolution, and systematics* 44 (2013): 51-72.
- Zhang, Jianzhi. "Neutral theory and phenotypic evolution." *Molecular biology and evolution* 35.6 (2018): 1327-1331.

APPENDIX A  
SUPPLEMENTARY TABLES

**Supplementary Table 1. Analysis of variance of growth-related traits in mutation-accumulation lines derived from ancestors in WT and MMR- genetic background.** Two traits are focused: maximum growth rate ( $\mu_{\max}$ ) and carrying capacity ( $K_c$ ). For each trait, the total variance is partitioned into three components: between-batch component ( $V_B$ ), among-line component ( $V_L$ ), and the residual environmental component ( $V_E$ ). The associated standard errors,  $SE(V_B)$ ,  $SE(V_L)$ , and  $SE(V_E)$ , and the associated degrees of freedom,  $DF_B$ ,  $DF_L$ , and  $DF_E$ , are also listed.  $P_B$  represents the  $P$ -value of the  $F$ -test for the significance of  $V_B$  compared to  $V_L$ .  $P_L$  represents the  $P$ -value of the  $F$ -test for the significance of  $V_L$  compared to  $V_E$ . Mutational variance ( $V_m$ ) of each trait and each genetic background is further estimated by  $2V_L/g$ , where  $g$  is the total generation number in the entire mutation-accumulation process. The associated standard errors,  $SE(V_m)$ , are also listed.

Trait	Ancestor	$V_B$	$SE(V_B)$	$DF_B$	$V_L$	$SE(V_L)$	$DF_L$	$V_E$	$SE(V_E)$	$DF_E$	$P_B$	$P_L$	$g$	$V_m$	$SE(V_m)$
$\mu_{\max}$	WT	-0.000053	0.000013	1	0.001198	0.00026	40	0.00018	0.0000086	911	0.78	$<1 \times 10^{-300}$	1712	$1.4 \times 10^{-6}$	$3.1 \times 10^{-7}$
$\mu_{\max}$	MMR-	-0.000373	0.000084	1	0.007272	0.00163	38	0.00091	0.0000434	875	0.94	$<1 \times 10^{-300}$	1639	$8.9 \times 10^{-6}$	$2.0 \times 10^{-6}$
$K_c$	WT	0.000013	0.000148	1	0.003281	0.00074	40	0.00220	0.0001027	911	0.31	$4 \times 10^{-155}$	1712	$3.8 \times 10^{-6}$	$9.0 \times 10^{-7}$
$K_c$	MMR-	0.000522	0.000890	1	0.010775	0.00243	38	0.00235	0.0001121	875	0.17	$7 \times 10^{-298}$	1639	$1.3 \times 10^{-5}$	$3.0 \times 10^{-6}$

**Supplementary Table 2. Analysis of variance of growth-related traits in mutation-accumulation lines whose progenitors were isolated from experimentally evolved populations.** Two traits are focused: maximum growth rate ( $\mu_{\max}$ ) and carrying capacity ( $K_c$ ). The schemes of experimental evolution for the populations that the MA progenitors come from are categorized by the genetic backgrounds of experimental evolution ancestors (WT or MMR-) and transfer sizes (Large or Small). For each MA experiment, the total variance is partitioned into two components: the among-line component ( $V_L$ ) and the residual environmental component ( $V_E$ ). The associated standard errors,  $SE(V_L)$  and  $SE(V_E)$ , and the associated degrees of freedom,  $DF_L$ , and  $DF_E$ , are also listed.  $P_L$  represents the  $P$ -value of the  $F$ -test for the significance of  $V_L$  compared to  $V_E$ . Mutational variance ( $V_m$ ) of each trait and each MA experiment is further estimated by  $2V_L/g$ , where  $g$  is the total generation number in the entire mutation-accumulation process. The associated standard errors,  $SE(V_m)$ , are also listed.

Trait	MA Progenitor	Experimental Evolution Scheme	$V_L$	$SE(V_L)$	$DF_L$	$V_E$	$SE(V_E)$	$DF_E$	$P_L$	$g$	$V_m$	$SE(V_m)$
$\mu_{\max}$	L1-C2	WT Large	0.0018	0.00051	23	0.00020	0.000015	342	$2 \times 10^{-157}$	1663	$2.1 \times 10^{-6}$	$6.1 \times 10^{-7}$
$\mu_{\max}$	L1-D1	WT Large	0.0310	0.01433	20	0.01306	0.000219	304	$5 \times 10^{-70}$	1463	$4.2 \times 10^{-5}$	$2.0 \times 10^{-5}$
$\mu_{\max}$	L1-D2	WT Large	0.0263	0.00959	23	0.01599	0.001024	323	$7 \times 10^{-58}$	1488	$3.5 \times 10^{-5}$	$1.3 \times 10^{-5}$
$\mu_{\max}$	S1-C1	WT Small	0.0061	0.00746	22	0.00365	0.001239	331	$5 \times 10^{-60}$	1659	$7.3 \times 10^{-6}$	$9.0 \times 10^{-6}$
$\mu_{\max}$	S1-C2	WT Small	0.0089	0.00143	22	0.00525	0.000017	316	$1 \times 10^{-57}$	1616	$1.1 \times 10^{-5}$	$1.8 \times 10^{-6}$
$\mu_{\max}$	L1-A1	MMR- Large	0.0494	0.00203	19	0.00271	0.000310	275	$1 \times 10^{-165}$	1626	$6.1 \times 10^{-5}$	$2.5 \times 10^{-6}$
$\mu_{\max}$	L1-B1	MMR- Large	0.0050	0.00262	23	0.00022	0.000409	328	$2 \times 10^{-212}$	1611	$6.2 \times 10^{-6}$	$3.3 \times 10^{-6}$
$\mu_{\max}$	S1-A1	MMR- Small	0.0028	0.00088	18	0.00015	0.000013	266	$2 \times 10^{-162}$	1565	$3.6 \times 10^{-6}$	$1.1 \times 10^{-6}$
$\mu_{\max}$	S1-B1	MMR- Small	0.0107	0.00381	14	0.00092	0.000092	194	$2 \times 10^{-99}$	1598	$1.3 \times 10^{-5}$	$4.8 \times 10^{-6}$
$K_c$	L1-C2	WT Large	0.0030	0.00085	23	0.00022	0.000017	342	$1 \times 10^{-185}$	1663	$3.6 \times 10^{-6}$	$1.0 \times 10^{-6}$
$K_c$	L1-D1	WT Large	0.1127	0.02536	20	0.02542	0.001272	304	$1 \times 10^{-100}$	1463	$1.5 \times 10^{-4}$	$3.5 \times 10^{-5}$
$K_c$	L1-D2	WT Large	0.0516	0.03443	23	0.03152	0.001994	323	$1 \times 10^{-57}$	1488	$6.9 \times 10^{-5}$	$4.6 \times 10^{-5}$
$K_c$	S1-C1	WT Small	0.0136	0.01461	22	0.00216	0.002443	331	$4 \times 10^{-130}$	1659	$1.6 \times 10^{-5}$	$1.8 \times 10^{-5}$
$K_c$	S1-C2	WT Small	0.0571	0.00220	22	0.00313	0.000067	316	$3 \times 10^{-190}$	1616	$7.1 \times 10^{-5}$	$2.7 \times 10^{-6}$

K <sub>c</sub>	L1-A1	MMR- Large	0.0867	0.00441	19	0.01573	0.000184	275	1×10 <sup>-101</sup>	1626	1.1×10 <sup>-4</sup>	5.4×10 <sup>-6</sup>
K <sub>c</sub>	L1-B1	MMR- Large	0.0076	0.01630	23	0.00085	0.000244	328	9×10 <sup>-151</sup>	1611	9.4×10 <sup>-6</sup>	2.0×10 <sup>-5</sup>
K <sub>c</sub>	S1-A1	MMR- Small	0.0069	0.00218	18	0.00061	0.000053	266	3×10 <sup>-134</sup>	1565	8.8×10 <sup>-6</sup>	2.8×10 <sup>-6</sup>
K <sub>c</sub>	S1-B1	MMR- Small	0.1401	0.04957	14	0.00196	0.000198	194	3×10 <sup>-172</sup>	1598	1.8×10 <sup>-4</sup>	6.2×10 <sup>-5</sup>

**Supplementary Table 3. Expectation of mutational effects and square mutational effects on growth-related traits in WT and MMR- ancestors.** For each of the two experimental evolution ancestors (WT and MMR-), the per-generation mutation rate ( $U$ ) has been calculated using mutational data from the MA experiments derived from the ancestors. For each of the two growth-related traits ( $\mu_{\max}$  and  $K_c$ ), the expectation of mutational effects ( $E(a)$ ) and the expectation of square mutational effects ( $E(a^2)$ ) were calculated using growth curve data and mutational data from the MA experiments derived from the WT and MMR- ancestors.

Trait	Ancestor	$U$	$E(a)$	$SE(E(a))$	$E(a^2)$	$SE(E(a^2))$
$\mu_{\max}$	WT	0.0019	$-1.2 \times 10^{-3}$	$1.6 \times 10^{-3}$	$7.2 \times 10^{-4}$	$1.6 \times 10^{-4}$
$\mu_{\max}$	MMR-	0.1329	$-5.4 \times 10^{-4}$	$1.0 \times 10^{-4}$	$6.7 \times 10^{-5}$	$1.5 \times 10^{-5}$
$K_c$	WT	0.0019	$3.3 \times 10^{-3}$	$2.7 \times 10^{-3}$	$2.0 \times 10^{-3}$	$4.4 \times 10^{-4}$
$K_c$	MMR-	0.1329	$-2.0 \times 10^{-4}$	$8.3 \times 10^{-5}$	$9.9 \times 10^{-5}$	$2.2 \times 10^{-5}$

**Supplementary Table 4. Expectation of mutational effects and square mutational effects on growth-related traits in experimentally evolved populations.** For each of the experimentally evolved populations, the per-generation mutation rate ( $U$ ) has been calculated using mutational data from the MA experiments derived from the clonal progenitors. The schemes of experimental evolution for the populations that the MA progenitors come from are categorized by the genetic backgrounds of experimental evolution ancestors (WT or MMR-) and transfer sizes (Large or Small). For each of the two growth-related traits ( $\mu_{\max}$  and  $K_c$ ), the expectation of mutational effects ( $E(a)$ ) and the expectation of square mutational effects ( $E(a^2)$ ) were calculated using growth curve data and mutational data from the MA experiments derived from the evolved populations.

Trait	MA Progenitor	Experimental Evolution Scheme	$U$	$E(a)$	$SE(E(a))$	$E(a^2)$	$SE(E(a^2))$
$\mu_{\max}$	L1-C2	WT Large	0.0030	$-3.5 \times 10^{-3}$	$1.8 \times 10^{-3}$	$7.1 \times 10^{-4}$	$2.0 \times 10^{-4}$
$\mu_{\max}$	L1-D1	WT Large	0.0019	$-1.9 \times 10^{-2}$	$1.3 \times 10^{-2}$	$2.2 \times 10^{-2}$	$1.0 \times 10^{-2}$
$\mu_{\max}$	L1-D2	WT Large	0.0027	$-8.1 \times 10^{-3}$	$8.4 \times 10^{-3}$	$1.3 \times 10^{-2}$	$4.8 \times 10^{-3}$
$\mu_{\max}$	S1-C1	WT Small	0.0029	$-9.8 \times 10^{-3}$	$3.9 \times 10^{-3}$	$2.5 \times 10^{-3}$	$3.1 \times 10^{-3}$
$\mu_{\max}$	S1-C2	WT Small	0.0029	$1.1 \times 10^{-2}$	$4.8 \times 10^{-3}$	$3.8 \times 10^{-3}$	$6.2 \times 10^{-4}$
$\mu_{\max}$	L1-A1	MMR- Large	0.1192	$-1.0 \times 10^{-4}$	$2.5 \times 10^{-4}$	$5.1 \times 10^{-4}$	$2.1 \times 10^{-5}$
$\mu_{\max}$	L1-B1	MMR- Large	0.1335	$-8.0 \times 10^{-4}$	$1.8 \times 10^{-4}$	$4.6 \times 10^{-5}$	$2.4 \times 10^{-5}$
$\mu_{\max}$	S1-A1	MMR- Small	0.0867	$-6.7 \times 10^{-4}$	$1.8 \times 10^{-4}$	$4.1 \times 10^{-5}$	$1.3 \times 10^{-5}$
$\mu_{\max}$	S1-B1	MMR- Small	0.0836	$-8.6 \times 10^{-4}$	$2.9 \times 10^{-4}$	$1.6 \times 10^{-4}$	$5.7 \times 10^{-5}$
$K_c$	L1-C2	WT Large	0.0030	$-3.5 \times 10^{-3}$	$2.4 \times 10^{-3}$	$1.2 \times 10^{-3}$	$3.4 \times 10^{-4}$
$K_c$	L1-D1	WT Large	0.0019	$-4.7 \times 10^{-3}$	$2.1 \times 10^{-2}$	$8.0 \times 10^{-2}$	$1.8 \times 10^{-2}$
$K_c$	L1-D2	WT Large	0.0027	$2.1 \times 10^{-2}$	$1.2 \times 10^{-2}$	$2.6 \times 10^{-2}$	$1.7 \times 10^{-2}$
$K_c$	S1-C1	WT Small	0.0029	$-1.8 \times 10^{-2}$	$6.1 \times 10^{-3}$	$5.6 \times 10^{-3}$	$6.0 \times 10^{-3}$
$K_c$	S1-C2	WT Small	0.0029	$2.8 \times 10^{-2}$	$1.2 \times 10^{-2}$	$2.5 \times 10^{-2}$	$9.6 \times 10^{-4}$
$K_c$	L1-A1	MMR- Large	0.1192	$5.3 \times 10^{-4}$	$3.5 \times 10^{-4}$	$8.9 \times 10^{-4}$	$4.5 \times 10^{-5}$
$K_c$	L1-B1	MMR- Large	0.1335	$-2.4 \times 10^{-4}$	$9.4 \times 10^{-5}$	$7.1 \times 10^{-5}$	$1.5 \times 10^{-4}$

K <sub>c</sub>	S1-A1	MMR- Small	0.0867	-5.8×10 <sup>-4</sup>	1.9×10 <sup>-4</sup>	1.0×10 <sup>-4</sup>	3.2×10 <sup>-5</sup>
K <sub>c</sub>	S1-B1	MMR- Small	0.0836	3.2×10 <sup>-4</sup>	7.0×10 <sup>-4</sup>	2.1×10 <sup>-3</sup>	7.4×10 <sup>-4</sup>

**Supplementary Table 5. Analysis of variance of growth-related traits in individual experimentally evolved populations of WT and MMR- genetic backgrounds and large and small transfer sizes.** Two traits are focused: maximum growth rate ( $\mu_{\max}$ ) and carrying capacity ( $K_c$ ). For each trait, the total variance is partitioned into two components: within-population component ( $V_W$ ), and the residual environmental component ( $V_E$ ). The associated standard errors,  $SE(V_W)$  and  $SE(V_E)$ , and the associated degrees of freedom,  $DF_W$  and  $DF_E$ , are also listed.  $P_W$  represents the  $P$ -value of the  $F$ -test for the significance of  $V_W$  compared to  $V_E$ . The increase of within-population variance per generation ( $V_W'$ ) of each population is further estimated by  $V_W/g$ , where  $g$  is the total generation number in the experimental evolution. The associated standard errors,  $SE(V_W')$ , are also listed.

Trait	Ancestor	Transfer Size	Population	$V_W$	$SE(V_W)$	$DF_W$	$V_E$	$SE(V_E)$	$DF_E$	$P_W$	$g$	$V_W'$	$SE(V_W')$
$\mu_{\max}$	WT	Large	L1-C	0.00093	0.00022	37	0.00032	0.000020	518	$8 \times 10^{-135}$	2990	$3.1 \times 10^{-7}$	$7.2 \times 10^{-8}$
$\mu_{\max}$	WT	Large	L1-D	0.01067	0.00249	35	0.00052	0.000033	504	$< 1 \times 10^{-300}$	2990	$3.6 \times 10^{-6}$	$8.3 \times 10^{-7}$
$\mu_{\max}$	WT	Small	S1-C	0.00226	0.00060	36	0.00540	0.000342	495	$1 \times 10^{-26}$	20900	$1.1 \times 10^{-7}$	$2.9 \times 10^{-8}$
$\mu_{\max}$	MMR-	Large	L1-A	0.01565	0.00361	36	0.00133	0.000083	507	$3 \times 10^{-260}$	2990	$5.2 \times 10^{-6}$	$1.2 \times 10^{-6}$
$\mu_{\max}$	MMR-	Large	L1-B	0.05372	0.01199	39	0.00844	0.000517	532	$1 \times 10^{-209}$	2990	$1.8 \times 10^{-5}$	$4.0 \times 10^{-6}$
$\mu_{\max}$	MMR-	Small	S1-A	0.01262	0.00290	39	0.00808	0.000478	570	$5 \times 10^{-98}$	20900	$6.0 \times 10^{-7}$	$1.4 \times 10^{-7}$
$\mu_{\max}$	MMR-	Small	S1-B	0.00437	0.00100	37	0.00061	0.000038	514	$1 \times 10^{-213}$	20900	$2.1 \times 10^{-7}$	$4.8 \times 10^{-8}$
$K_c$	WT	Large	L1-C	0.00163	0.00040	37	0.00211	0.000131	518	$4 \times 10^{-50}$	2990	$5.4 \times 10^{-7}$	$1.3 \times 10^{-7}$
$K_c$	WT	Large	L1-D	0.00710	0.00167	35	0.00134	0.000084	504	$2 \times 10^{-182}$	2990	$2.4 \times 10^{-6}$	$5.6 \times 10^{-7}$
$K_c$	WT	Small	S1-C	0.01627	0.00378	36	0.00319	0.000202	495	$3 \times 10^{-175}$	20900	$7.8 \times 10^{-7}$	$1.8 \times 10^{-7}$
$K_c$	MMR-	Large	L1-A	0.01314	0.00306	36	0.00286	0.000179	507	$2 \times 10^{-170}$	2990	$4.4 \times 10^{-6}$	$1.0 \times 10^{-6}$
$K_c$	MMR-	Large	L1-B	0.11103	0.02455	39	0.00176	0.000108	532	$< 1 \times 10^{-300}$	2990	$3.7 \times 10^{-5}$	$8.2 \times 10^{-6}$
$K_c$	MMR-	Small	S1-A	0.04504	0.00997	39	0.00154	0.000091	570	$< 1 \times 10^{-300}$	20900	$2.2 \times 10^{-6}$	$4.8 \times 10^{-7}$
$K_c$	MMR-	Small	S1-B	0.01785	0.00405	37	0.00071	0.000044	514	$< 1 \times 10^{-300}$	20900	$8.5 \times 10^{-7}$	$1.9 \times 10^{-7}$